

# Lopsided spiral galaxies

Chanda J. Jog\* & Francoise Combes\*\*

\* *Department of Physics, Indian Institute of Science, Bangalore 560012, India*

\*\* *Observatoire de Paris, LERMA, 61 Av. de l'Observatoire, Paris F-75014, France*

1

---

## Abstract

The light distribution in the disks of many galaxies is non-axisymmetric or ‘lopsided’ with a spatial extent much larger along one half of a galaxy than the other, as in M101. Recent near-IR observations show that lopsidedness is common. The stellar disks in nearly 30 % of galaxies have significant lopsidedness of  $> 10\%$  measured as the Fourier amplitude of the  $m=1$  component normalized to the average value. This asymmetry is traced particularly well by the atomic hydrogen gas distribution lying in the outer parts. The lopsidedness also occurs in the nuclear regions, where the nucleus is offset with respect to the outer isophotes. The galaxies in a group environment show higher lopsidedness. The origin of lopsidedness could be due to the disk response to a tidally distorted halo, or via gas accretion. An  $m=1$  perturbation in a disk leads to a shift in the center of mass in the disk, and this then acts as an indirect force on the original center of the disk. The disk is inherently supportive of an  $m=1$  mode, which is a particular feature only of lopsided modes, and which makes their dynamical study interesting and challenging.

The lopsidedness has a large impact on the dynamics of the galaxy, its evolution, the star formation in it, and on the growth of the central black hole and on the nuclear fueling, merging of binary black holes etc. The disk lopsidedness can be used as a diagnostic to study the halo asymmetry. This is an emerging area in galactic structure and dynamics. In this review, the observations to measure the lopsided distribution, as well as the theoretical progress made so far to understand its origin and properties, and the related open problems will be discussed.

*Key words:* galaxies : kinematics and dynamics - galaxies : ISM - galaxies : spiral - galaxies : structure - galaxies : individual: M101

---



---

<sup>1</sup> Corresponding author: Chanda J. Jog (email: [cjjog@physics.iisc.ernet.in](mailto:cjjog@physics.iisc.ernet.in))

## **Contents:**

1. Introduction
2. Observations of lopsidedness in galactic disks
  - 2.1 Morphological lopsidedness
    - 2.1.1 Morphological lopsidedness in HI gas
    - 2.1.2 Morphological lopsidedness in old stars
  - 2.2 Kinematical lopsidedness
  - 2.3 Phase of the disk lopsidedness
  - 2.4 Observations of off-centered nuclear disks
    - 2.4.1 The case of the M31 nuclear disk
    - 2.4.2 Other off-centered nuclei
3. Theoretical models for the origin of lopsidedness
  - 3.1 Kinematical model for the origin of lopsidedness
  - 3.2 Dynamical models for the origin of lopsidedness
    - 3.2.1 Tidal encounters, and disk response to distorted halo
      - 3.2.1.a Orbits and isophotes in a perturbed disk
      - 3.2.1.b Kinematics in a perturbed disk
      - 3.2.1.c Radius for the onset of lopsidedness
      - 3.2.1.d Comparison of  $A_1$  vs. Tidal parameter
    - 3.2.2 Gas Accretion, and other mechanisms
    - 3.2.3 Lopsidedness as a global instability
    - 3.2.4 Effect of inclusion of rotation and a live halo
  - 3.3 Comparison between origin of  $m=1$  and  $m=2$ , stars and gas
  - 3.4 A summary of the various mechanisms
4. Lopsidedness in the central region

- 4.1 Stability of central nuclear disks
  - 4.1.1 Slow stable modes, damping slowly
- 4.2 Double nuclei due to infalling bodies
- 4.3 Core wandering
- 4.4 Other mechanisms
- 5. Lopsidedness in galaxies in groups, clusters, and mergers
  - 5.1 Lopsidedness in galaxies in groups
  - 5.2 Lopsidedness in galaxies in clusters
  - 5.3 Lopsidedness in centers of advanced mergers
- 6. Related topics
  - 6.1 Relative strengths of lopsidedness ( $m=1$ ) and spiral arms/bars ( $m=2$ )
    - 6.1.1 Observed amplitudes of  $m=1$  and  $m=2$  components
  - 6.2 Asymmetry in the dark matter halo
  - 6.3 Comparison with warps
  - 6.4 Implications for high redshift galaxies
- 7. Effect of lopsidedness on galaxy evolution
- 8. Summary & future directions

## 1 Introduction

It has been known for a long time that the light and hence the mass distribution in disks of spiral galaxies is not strictly axisymmetric, as for example in M 101 or in NGC 1637 (Sandage 1961), where the isophotes are elongated in one half of the galaxy. Despite this, however, astronomers have largely tended to ignore this fact and to assume the disks to be axisymmetric because it is much simpler to study the dynamics of axisymmetric disks. This phenomenon was first highlighted in the pioneering paper by Baldwin, Lynden-Bell, & Sancisi (1980), where they detected an asymmetry in the spatial extent of the atomic hydrogen gas in the outer regions in the two halves of some galaxies, and gave these the apt name of ‘lopsided’ galaxies. A galaxy is said to be lopsided if it displays a global non-axisymmetric spatial distribution of type  $m = 1$  where  $m$  is the azimuthal wavenumber, or a  $\cos\phi$  distribution where  $\phi$  is the azimuthal angle in the plane of the disk.

Surprisingly no further systematic work was done on this topic till mid-1990’s. Since then there has been a resurgence in this field. The lopsided distribution has now been detected and studied also in the old stellar component as traced in the near-IR starting with the observations of Block et al. (1994) and Rix & Zaritsky (1995). This exciting new development of the imaging studies of spiral galaxies in the near-IR K-band ( $2.2\ \mu$ ) was made possible by the development of the NICMOS 3 array. The dust extinction effects are negligible in the near-IR, hence these studies reveal the spatial distribution of the underlying old stellar population, which constitute the main mass component of the disk. These observations detected a non-axisymmetric  $m = 1$  distribution of surface density of old stars in the inner/optical region of the disk. Rix & Zaritsky (1995) define  $A_1$ , the fractional amplitude of the first azimuthal Fourier component ( $m = 1$ ) of surface brightness, to be the quantitative measure of disk lopsidedness. They find that  $A_1$  increases with radius. The average value measured between 1.5-2.5 disk scalelengths is large  $\geq 0.1$ , and 30% of the galaxies studied show a higher lopsidedness (Zaritsky & Rix 1997). A similar high average value of disk lopsidedness was confirmed in a recent Fourier-analysis study of a much larger sample of 149 galaxies (Bournaud et al. 2005 b).

The above analysis shows that nearly one third of the 149 galaxies exhibit 10 % or more asymmetry in the amplitude of the  $m = 1$  Fourier component. Thus, *lopsided distribution in the disk is a general phenomenon*, and is stronger at larger radii. Hence it is important to understand the origin and dynamics of the lopsided distribution in spiral galaxies.

The lopsided distribution in the HI gas has been mapped spatially (Haynes et al. 1998), and also mapped kinematically for a few galaxies (Schoenmakers,

Franx & de Zeeuw 1997, Swaters et al. 1999), and by global velocity profiles for a much larger sample (Richter & Sancisi 1994). Such an asymmetry has also been detected in dwarf galaxies (Swaters et al. 2002), and also in the star-forming regions in irregular galaxies (Heller et al. 2000). The asymmetry may affect all scales in a galaxy. While the large-scale lopsidedness is more conspicuous, the off-centering of nuclei is now often discovered at high spatial resolution. A prototype of this  $m = 1$  nuclear distribution is the inner region of M31, where the central black hole is clearly off-centered with respect to its nuclear stellar disk (e.g., Tremaine 2001). This frequent nuclear  $m = 1$  perturbation must play a central role in the fueling of the active galactic nucleus (AGN) in a galaxy.

The origin and the evolution of lopsidedness are not yet well-understood, though a beginning has been made to address these problems theoretically. Like any other non-axisymmetric perturbation, the lopsided distribution would also tend to get wound up by the differential rotation in the galactic disk within a few dynamical timescales. Since a large fraction of galaxies exhibit lopsidedness, it must be either a long-lived phenomenon or generated frequently. Tidal interaction (Beale & Davies 1969), and satellite galaxy accretion (Zaritsky & Rix 1997) have been suggested as the origin of the disk lopsidedness, these can occur frequently. Weinberg (1995) has shown that the tidal interaction between the Galaxy and the Large Magellanic Cloud (LMC) leads to a lopsided distortion of the Galaxy halo at resonance points between the LMC and the halo orbit frequencies, which in turn causes a lopsided distribution in the disk of the Galaxy. Since galaxy interactions are now known to be common, the origin of disk lopsidedness as attributed to the disk response to the tidal distortion in a halo has been proposed and studied by Jog (1997, 2002), and Schoenmakers et al. (1997). Some other possible mechanisms that have been suggested involve an off-center disk in a halo as in a dwarf galaxy (Levine & Sparke 1998), or gas accretion (Bournaud et al. 2005 b), or treating it as a global, long-lived mode (Saha, Combes & Jog 2007).

The  $m = 1$  distribution in the inner regions of some galaxies such as M 31 has been modeled through analytical work and numerical simulations (Tremaine 1995, Statler 2001, Bacon et al. 2001, de Oliveira & Combes 2008). According to the various physical conditions in galaxy nuclei (such as the mass of the bulge, the mass of the nuclear disk and that of the central black hole, the presence of gas, etc.), an  $m = 1$  mode is unstable, or an  $m = 1$  excitation is very slowly damped and can persist for several hundreds of dynamical times. Such long-lived lopsided distribution is also seen in the centers of advanced mergers of galaxies (Jog & Maybhat 2006). Due to their persistence, the lopsided modes could play a significant role in the evolution of the central regions of galaxies, especially in the fueling of a central AGN.

An  $m=1$  perturbation in a disk leads to a shift in the center of mass in the disk,

and this then acts as an indirect force on the original center of the disk. The disk is inherently supportive of an  $m=1$  mode, which is a particular feature only of a lopsided mode. This results in long-lasting global lopsided modes. While the  $m = 2$  case corresponding to the two-armed spiral pattern or bars has been studied extensively, the  $m = 1$  mode has not received comparable attention in the literature so far. This has to be redressed: first,  $m=1$  is common and the amplitude is even larger than for  $m=2$  (Jarrett et al. 2003), second, the  $m=1$  modes do not have an Inner Lindblad Resonance, or ILR (e.g., Block et al. 1994), and hence can allow transport of matter in the inner regions, and third, these appear to be long-lived.

The existence of long-lived lopsided modes is expected to have a significant impact on the dynamics of the galaxy, the star formation in it, and on the nuclear fueling etc. In the tidal picture, the disk lopsidedness can be used as a diagnostic to study the lopsidedness of the dark matter halo (Jog 1999). Similarly, higher-order ( $m = 2$ ) disk asymmetry can allow one to study the ellipticity of the dark matter halo (Jog 2000, Andersen & Bershadsky 2002). Thus in addition to being interesting and challenging in itself, a study of disk lopsidedness can yield information about a number of other interesting properties of galaxies. Extra-planar gas and lopsidedness are frequently correlated (Sancisi et al 2008).

Recently, the lopsided distribution in galaxies in different environments such as groups and clusters and centers of mergers has been studied. These show different properties, such as the higher observed lopsided amplitudes in the group galaxies (Angiras et al. 2006). In future studies, these can act as important tracers of the dynamics of disks and dark matter halos in these settings.

In Section 2, we discuss the observational properties of lopsidedness as seen in HI and old stars, in the main disk as well as in the central region of galaxies. The various theoretical models proposed in the literature and their comparison is given in Section 3. The dynamics of lopsidedness in the central region of the near-Keplerian case region is discussed in Section 4. Section 5 discusses the observations and dynamical implications of lopsidedness in galaxies in a different setting, namely in groups, clusters and in centers of mergers. Section 6 discusses several related points including the comparison between  $m=1$  and 2 cases, the deduction of the halo asymmetry etc. Section 7 gives the effect of lopsidedness on the galaxy. Finally, Section 8 gives a brief summary and future directions for this field.

## 2 Observations of lopsidedness in galactic disks

While lopsidedness is seen to be a ubiquitous phenomenon (Section 1), various methods are used in the literature to define the asymmetry in disk galaxies. We list and compare below the details, such as the definitions, the size of the sample studied, the tracer used (near-IR radiation from old stars, and 21 cm emission from the HI gas etc.) There is no consensus so far as to what is the definition for lopsidedness as well as what constitutes lopsidedness (or the threshold). Obviously this has to be done if say the percentage of galaxies showing lopsidedness as per the different criteria are to be compared. At the end of Section 2.1, we recommend the use of a standard criterion for lopsidedness as well as the threshold that could be adopted by future workers.

The disk lopsidedness in spiral galaxies has been studied in two different tracers- HI, the atomic hydrogen gas studied in the outer parts of disks, and the near-IR radiation from the inner/optical disks which traces the old stellar component of the disks. The lopsidedness was historically first detected in the HI, which we now realize is due to a higher lopsided amplitude at large radii. Hence we follow the same, chronological order in the summary of observations given next.

### 2.1 *Morphological lopsidedness*

#### 2.1.1 *Morphological lopsidedness in HI gas*

The asymmetric distribution of HI in M101 was noted in the early HI observations (Beale & Davies 1969). This phenomenon was first highlighted by Baldwin et al. (1980), who studied galaxies with highly asymmetric spatial extent of atomic hydrogen gas distributions in the outer regions in the two halves of a galaxy, such as M101 and NGC 2841 (see Fig. 1 here). This paper mentions the asymmetric distribution of light and HI in spiral galaxies such as M101. Quantitatively, they looked at the HI distribution in the four prototypical galaxies, namely, M101, NGC 891, NGC 4565, NGC 2841. They defined a galaxy to be "lopsided" in which the galaxy is more extended on one side than the other, and where the projected density of HI on the two sides of the galaxy is at least 2:1, and in which the asymmetry persists over a large range in radius and position angle. All these lopsided galaxies were also noted to have large-scale velocity perturbations. For a quantitative measurement of lopsidedness the edge-on systems cannot be used. The cut-off in inclination used for the near-IR and HI studies is given in Sections 2.1.2 and 5.1 respectively.

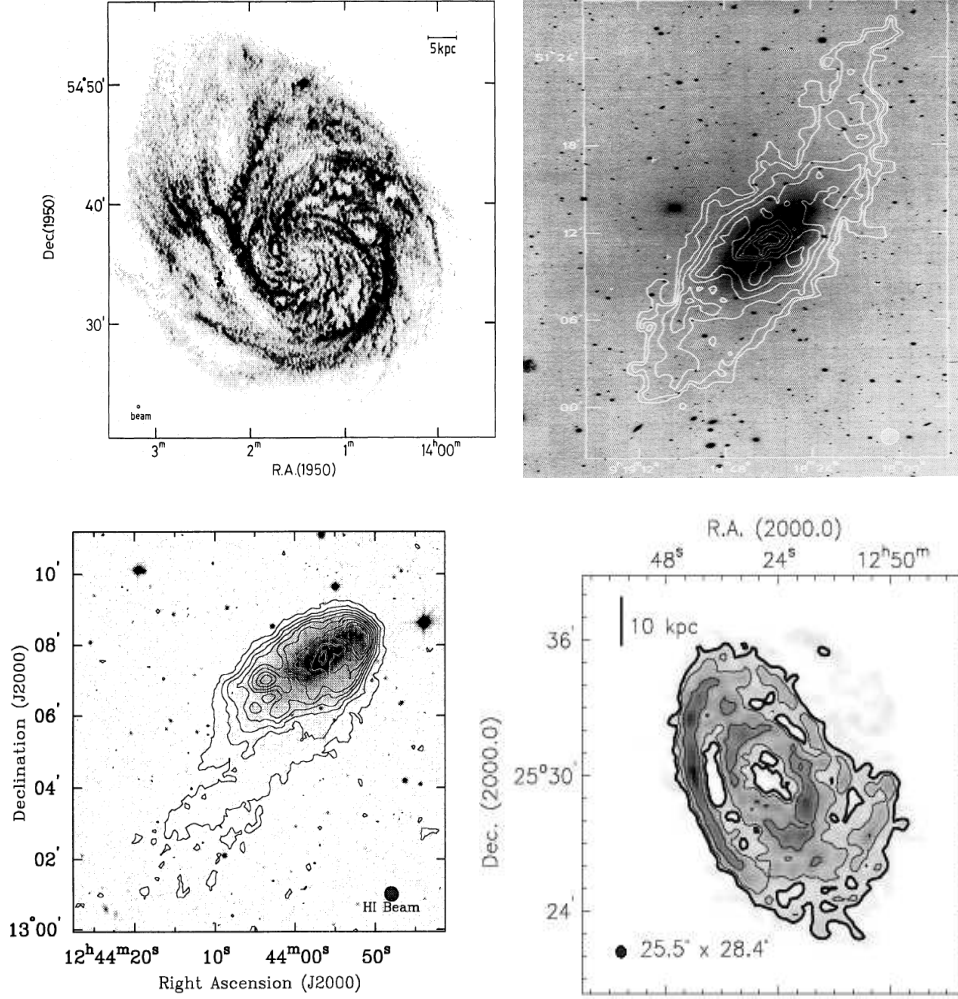


Fig. 1. Galaxies showing an asymmetry in the spatial extent of 2:1 or more in the HI distribution : M101 (top left, where the HI intensity is plotted here as gray scale) and NGC 2841 (top right: here the HI contours are superimposed on an optical image), These galaxies were termed "lopsided" galaxies by Baldwin, Lynden-Bell, & Sancisi (1980). These figures are from Braun (1995) and Bosma (1981) respectively. Other typical examples are NGC 4654 (lower left: where HI contours are superimposed on an optical image) and UGC7989 (lower right, showing contours and grey scale of the HI intensity), from Phookun & Mundy (1995), and Noordermeer et al. (2005) respectively.

There was no further work on this topic for over a decade. Further HI mapping of a few individual galaxies such as NGC 4254 was done by Phookun, Vogel, & Mundy (1993) which stressed the obvious spatial asymmetry but they did not measure the lopsidedness. This paper studied the special case of the not-so-common one-armed galaxies such as NGC 4254 where the phase varies with radius (see Section 2.3).



Richter & Sancisi (1994) collected data from single-dish HI surveys done using different radio telescopes, for a large sample of about 1700 galaxies. They found that 50 % of galaxies studied show strong lopsidedness in their global HI velocity profiles. This could be either due to spatial lopsided distribution and/or lopsided kinematics. But since a large fraction of their sample shows this effect, they concluded that it must reflect an asymmetry in the gas density, as is confirmed by the correlation between the spatial and global HI velocity asymmetries in some galaxies like NGC 891, see Fig. 2 here. They argued that the asymmetry in HI represents a large-scale structural property of the galaxies. The criteria they used to decide the asymmetry are: (1). significant flux difference between the two horns ( $> 20\%$  or  $> 8$  sigma) (2). Total flux difference ( $> 55 : 45\%$ ) between the low and the high velocity halves (3). Width differences in the two horns ( $> 4$  velocity channels or  $50 \text{ km s}^{-1}$ ). One word of caution is that it is not clear from their paper if these three give consistent identification of a galaxy as being lopsided or not.

The global velocity tracer is likely to underestimate the asymmetry fraction as for example if the galaxy were to be viewed along the major axis as pointed out by Bournaud et al. (2005 b), or for a face-on galaxy as noted by Kamphuis (1993).

The comparison of asymmetry in the stars as detected in the near-IR and the HI asymmetry in surface density using the second criterion of Richter & Sancisi (1994) shows a similar behaviour in a sample of 76 galaxies (Fig. 6 of Bournaud et al. 2005 b). However, the asymmetry is quantitatively larger and more frequent in HI than in stars. This result supports the conjecture by Richter & Sancisi (1994) that the asymmetry in the global velocity profiles is a good tracer of the disk mass asymmetry. While making this comparison, it should be noted, however, that the HI asymmetry is seen more in the outer radial range while the asymmetry in the near-IR is seen in the inner region of a galactic disk.

Haynes et al. (1998) studied the global HI profiles of 103 fairly isolated spirals. 52 of the 78 or  $\sim 75\%$  galaxies showed statistically significant global profile asymmetry of 1.05. Many show large asymmetry: 35 have asymmetry  $> 1.1$ , 20 have  $> 1.15$ , and 11 have  $> 1.2$ .

The atomic hydrogen gas is an ideal tracer for a quantitative study of lopsidedness in galaxies since the HI gas extends farther out than the stars. The typical radial extent of HI is 2-3 times that of the stars (e.g. Giovanelli & Haynes 1988), and the amplitude of asymmetry increases with radius (Rix & Zaritsky 1995) as seen for the stars. However, surprisingly, a quantitative measurement of HI spatial lopsidedness has not been done until recently. In a first such study, the two-dimensional maps of the surface density of HI have

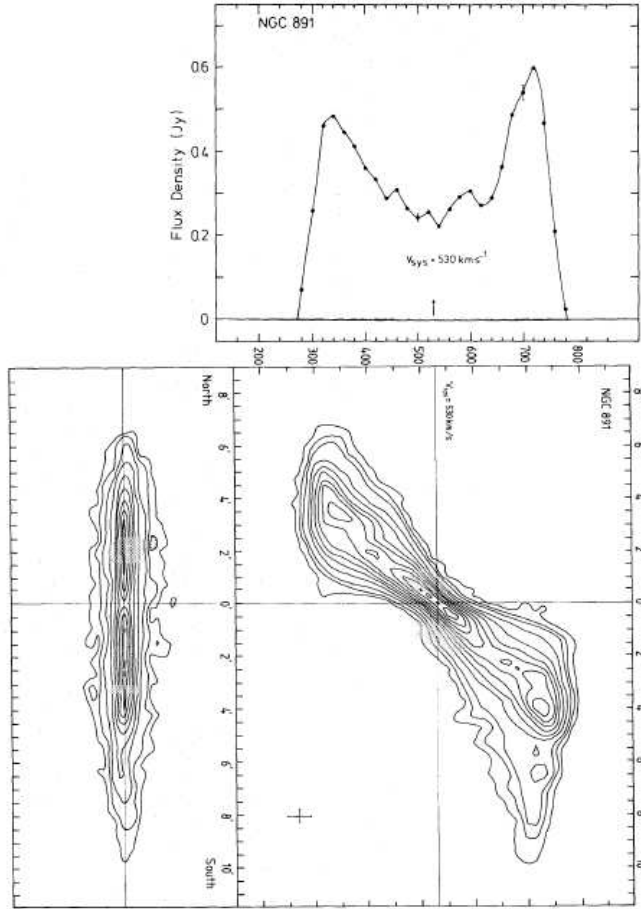


Fig. 2. Asymmetric HI surface density plot of NGC 891 (contours at the bottom left); position-velocity diagram of the same galaxy (contours at the bottom right); and the global velocity profile in NGC 891 (spectrum at the top), from Richter & Sancisi (1994).

been Fourier-analyzed recently to obtain the  $m=1$  Fourier amplitudes and phases for a sample of 18 galaxies in the Eridanus group (Angiras et al. 2006)-see Section 5.2 for details. Such analysis needs to be done for nearby, large-angular size galaxies using sensitive data which will allow a more detailed measurement of lopsidedness in nearby galaxies. A study along these lines is now underway using the data from WHISP, the Westerbork observations of neutral Hydrogen in Irregular and SPiral galaxies (Manthey et al. 2008).

The molecular hydrogen gas also shows a lopsided distribution in some galaxies, with more spatial extent along one half of a galaxy as in NGC 4565 (Richmond & Knapp 1986), IC 342 (Sage & Solomon 1991), NGC 628 (Adler & Liszt 1989) and M51 (Lord & Young 1990). However, this effect is not common in most cases and that can be understood as follows. The lopsidedness appears to be more strongly seen in the outer parts of a galaxy and the amplitude increases with radius as seen in stars (Rix & Zaritsky 1995), and also

in HI gas (Angiras et al. 2006). Theoretically it has been shown that the disk lopsidedness if arising due to a response to a distorted halo with a constant amplitude can only occur in regions beyond  $\sim 2$  disk scalelengths (Jog 2000). In most galaxies the molecular gas is constrained to lie within two disk scalelengths or half the optical radius (Young 1990). Hence we can see that in most galaxies, there is no molecular gas in the regions where disk lopsidedness in stars or HI is seen. This is why the molecular gas being in the inner parts of the galactic disk does not display lopsidedness in most cases.

### 2.1.2 *Morphological lopsidedness in old stars*

The near-IR traces the emission from the old stars since dust extinction does not significantly affect the emission in the near-IR. The systematic study of this topic was started in the 1990's when a few individual galaxies such as NGC 2997 and NGC 1637 were mapped in the near-IR by Block et al (1994). They noted the  $m=1$  asymmetry in these but did not study it quantitatively. The pioneering quantitative work in this field was done by Rix & Zaritsky (1995) who measured the asymmetry in the near-IR for a sample of 18 galaxies. In each galaxy,  $A_1$ , the fractional amplitude for the  $m=1$  mode normalized by an azimuthal average (or  $m=0$ ), was given at the outermost point measured in the disk, i.e. at 2.5 exponential disk scalelengths. This distance is set by the noise due to the sky background in the near-IR. The mean value is 0.14, and 30 % have  $A_1$  values more than 0.20 which were defined by them to be lopsided galaxies. A typical example is shown in Fig. 3.

This study was extended for a sample of 60 galaxies by Zaritsky & Rix (1997). They carried out the Fourier analysis of the near-IR surface brightness between the radial range of 1.5-2.5  $R_{exp}$ , where  $R_{exp}$  is the characteristic scale of the exponential light distribution. The normalised  $m = 1$  Fourier amplitude  $A_1$  is a more representative indicator of disk lopsidedness.

It was shown that 30 % of the galaxies have  $A_1 > 0.2$ , which was taken to define the threshold lopsidedness as in the previous work. Rudnick & Rix (1998) studied 54 early-type galaxies (S0-Sab) in R- band and found that 20 % show  $A_1$  values measured between the radial range of 1.5-2.5  $R_{exp}$  to be  $> 0.19$ .

A similar measurement has recently been done on a much larger sample of 149 galaxies from the OSU (Ohio State University) database in the near-IR (Bournaud et al. 2005 b), see Fig. 4. This confirms the earlier studies but for a larger sample, and gives a smaller value of lopsided amplitude, namely  $\sim 30\%$  show lopsidedness amplitude of 0.1 or larger when measured over the radial range of 1.5-2.5  $R_{exp}$ . The galaxies with inclination angles of  $< 70^\circ$  were used

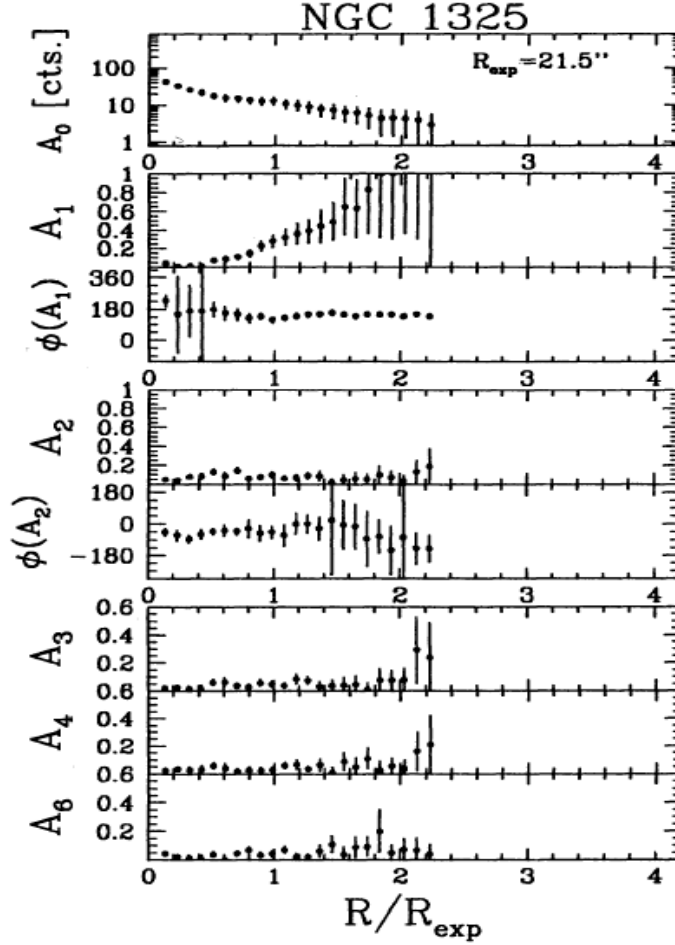


Fig. 3. The values of the various fractional Fourier amplitudes and phases vs. radius in units of the disk scalelengths for NGC 1325 (from Rix & Zaritsky 1995). The amplitude scale in the lower three panels has been expanded by a factor of 5/3 for clarity, since these higher  $m$  components have smaller amplitudes. The lopsided amplitude  $A_1$  increases with radius, and the phase is nearly constant with radius.

for this study. Since this is a large, unbiased sample it can be taken to give definitive values, and in particular the mean amplitude of 0.1 can be taken as the threshold value for deciding if a galaxy is lopsided. The lopsidedness also shows an increasing value with radius, as seen in the Rix & Zaritsky (1995) study.

In the Fourier decomposition studies the determination of the center is a tricky issue, and the same center has to be used for all the subsequent annular radial bins, otherwise during the optimization procedure, a different center could get chosen and will give a null measurement for the lopsidedness. This is applicable for the lopsidedness analysis for HI (Angiras et al. 2006, 2007), and also for centers of mergers (Jog & Maybhat 2006). These two cases are discussed

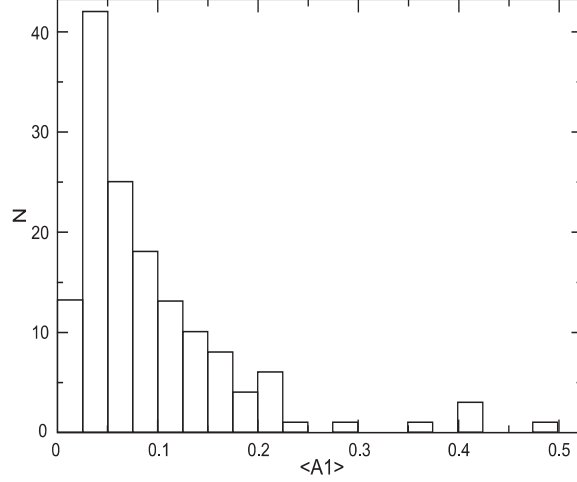


Fig. 4. The histogram showing the distribution of lopsidedness measured in 149 galaxies at inclination of  $< 70^\circ$  from the OSU sample (Bournaud et al. 2005 b). The typical normalized lopsided amplitude  $A_1$  measured over the radial range between 1.5 to 2.5 disk scalelengths is  $\sim 0.1$ . Thus most spiral galaxies show significant lopsidedness.

respectively in Sections 5.1 and 5.3.

The large number of galaxies used allows for a study of the variation with type. It is found that late-type galaxies are more prone to lopsidedness, in that a higher fraction of late-type galaxies are lopsided, and they show a higher value of the amplitude of lopsidedness (Bournaud et al. 2005 b), see Fig. 5. This is similar to what was found earlier for the variation with galaxy type for the HI asymmetries (Matthews, van Driel, & Gallagher 1998). These samples largely consist of field galaxies, while the group galaxies show a reverse trend with galaxy type (Angiras et al. 2006, 2007) implying a different mechanism for the origin of lopsidedness in these two settings, see Section 5.1 .

While an axisymmetric galaxy disk gives rise only to radial gravity forces, and therefore no torque, any asymmetry in the disk, either  $m = 1$ ,  $m = 2$  or higher, gives rise to tangential forces in addition to radial forces, and then to a gravity torque. From the near-infrared images, representative of old stars, and thus of most of the mass, it is possible to compute the gravitational forces experienced in a galactic disk. The computation of the gravitational torque presents important complementary information, namely it gives the overall average strength of the perturbation potential as shown for  $m=2$  (Block et al. 2002), and for  $m=1$  (Bournaud et al. 2005 b), whereas the Fourier amplitudes give values which are weighted more locally. The gravitational potential is derived from the near-infrared image, see Bournaud et al. (2005 b) for the details of this method. The  $m=1$  component of the gravitational torque,  $Q_1$  between 1.5-2.5 disk scalelengths is obtained, the histogram showing its

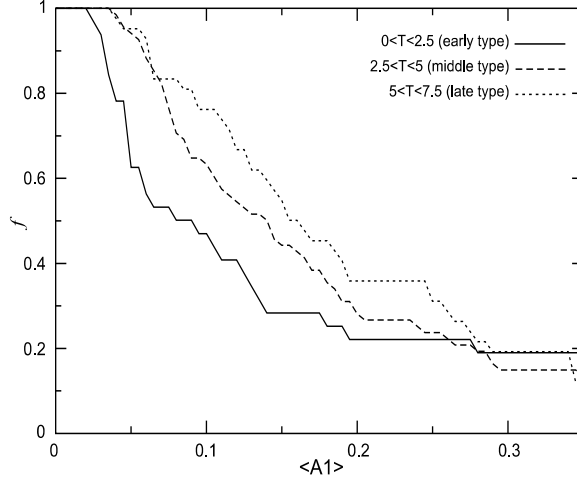


Fig. 5. The plot of the cumulative function of  $\langle A_1 \rangle$  for three groups of Hubble types of spiral galaxies: the early-types ( $0 < T < 2.5$ ), the intermediate types ( $2.5 < T < 5$ ), and the late-types ( $5 < T < 7.5$ ), where  $T$  denoted the Hubble type of a galaxy (taken from Bournaud et al. 2005 b). The late-type galaxies are more lopsided than the early-type galaxies.

distribution is plotted in Fig. 6, which is similar to that for the lopsided amplitude  $A_1$  (Fig. 4) as expected.

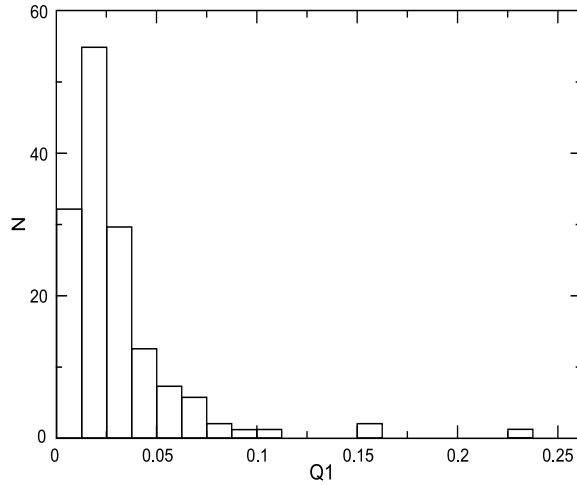


Fig. 6. The histogram of  $Q_1$ , the  $m=1$  Fourier amplitude in the gravitational potential, for the OSU sample of galaxies, from Bournaud et al. 2005 b.

An even larger sample based on the SDSS data has now been Fourier-analyzed by Reichard et al. (2008), and they also get a similar average value of lopsidedness in spiral galaxies, see Fig. 7. However, they use the surface density data between 50% and 90% light radii, so a clear one-to-one quantitative comparison of the values of lopsidedness from this work as compared to the previous papers in the literature discussed above is not possible. This work confirms

that galaxies with low concentration, and low stellar mass density (or the late-type spirals) are more likely to show lopsidedness, as shown earlier for HI by Matthews et al. (1998) and for stars by Bournaud et al. (2005 b).

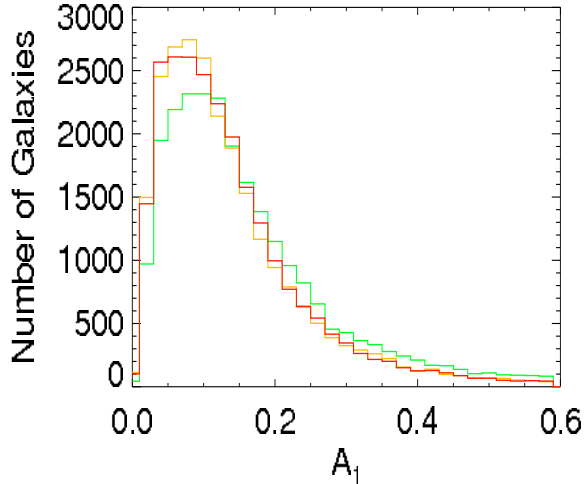


Fig. 7. The histogram of number of galaxies vs.  $A_1$  values for the SDSS sample, from Reichard et al. (2008). The histogram gives similar values to the earlier studies by Rix & Zaritsky (1995) and Bournaud et al. (2005 b)

Another approach to measure the asymmetry involves the wedge method (Kornreich et al. 1998, 2002) where the flux within circular sectors or wedges arranged symmetrically with respect to the galactic disk centre are compared. While it is easier to measure this than the Fourier amplitudes, it gives only average values. An extreme limit of the wedge method is applied by Abraham et al. (1996) and Conselice et al. (2000). They define the rotation asymmetry parameter as the ratio of fractional difference between the two sides, so that 0 corresponds to a symmetric galaxy and 0.5 for the most asymmetric galaxy. This is a more global or average definition of the disk asymmetry and is suitable for studying highly disturbed galaxies, and not those showing a systematic variation as in a lopsided distribution. Such highly disturbed systems are seen at high redshifts, for which this criterion was used first.

An interesting point to note is that spurious signs of asymmetry arising due to dust extinction (Rudnick & Rix 1998) and that arising due to the pointing error of single-dish telescope (Richter & Sancisi 1994) were checked and ruled out. Conversely, a galaxy could look more symmetric in the global velocity profile than it is, if the galaxy is seen face-on. In that case even though the morphology is asymmetric -as in HI in NGC 628, the global velocity profile is symmetric, and hence the galaxy would appear to be kinematically symmetric-see Kamphuis (1993).

Based on the above discussion of the various methods, we recommend that the

future users adopt the fractional Fourier amplitude  $A_1$  as the standard criterion for lopsidedness. This is because it gives a quantitative measurement, is well-defined, and can be measured easily as a function of radius in a galaxy, and thus allows an easy comparison of its value between galaxies and at different radii. The threshold value that could be adopted could be the average value of 0.1 seen in the field galaxies in the intermediate radial range of 1.5-2.5  $R_{exp}$  (Bournaud et al. 2005 b), so that galaxies showing a higher value can be taken to be lopsided. A uniform criterion will enable the comparison of amplitudes of lopsidedness in different galaxies, and also allow a comparison of the fraction of galaxies deduced to be lopsided in different studies.

## 2.2 *Kinematical lopsidedness*

The lopsidedness or a ( $\cos \phi$ ) asymmetry is often also observed in the kinematics of the galaxies. This could be as obvious as the asymmetry in the rotation curves on the two halves of a galactic disk, as is shown in Fig 8 (Swaters et al. 1999, Sofue & Rubin 2001), or more subtle as in the asymmetry in the velocity fields (Schoenmakers et al. 1997). Often the optical centres are distinctly separated spatially from the kinematical centers as in M33, M 31, and especially in dwarf galaxies as pointed out by Miller & Smith (1992). The rotation curve asymmetry is also seen as traced in the optical for stars (Sofue & Rubin 2001). The detailed 2-D velocity fields were so far mainly observed for HI as in the interferometric data (see e.g. Schoenmakers et al. 1997, Haynes et al. 1998). Now such information is beginning to be available for the bright stellar tracers as in  $H_\alpha$  emission from HII regions (Chemin et al. 2006, Andersen et al. 2006), however since the filling factor of this hot, ionized gas is small, it is not an ideal tracer for a quantitative study of disk lopsidedness.

Schoenmakers et al. (1997) use the kinematical observational data in HI on two galaxies- NGC 2403 and NGC 3198, and deduce the upper limit on the asymmetry in the  $m=2$  potential to be  $< a$  few percents. However, this method gives the result up to the sine of the viewing angle. Kinematic asymmetry in individual galaxies such as NGC 7479 has been studied and modeled as a merger with a small satellite galaxy (Laine & Heller 1999).

The rotation curve is asymmetric in the two halves of a galaxy or on the two sides of the major axis as shown for DDO 9 and NGC 4395 by Swaters et al. (1999), see Figure 8. However, they do not make a more detailed quantitative measurement of the asymmetry. Swaters (1999) in his study of dwarf galaxies showed that 50% of galaxies studied show lopsidedness in their kinematics. Schoenmakers (2000) applied his calculations on kinematical lopsidedness in galactic disks to five galaxies in the Sculptor group and found that all five show significant lopsidedness. A similar result has been found for the 18 galaxies



studied in the Ursa Major cluster (Angiras et al. 2007). The frequency of asymmetry and its magnitude is higher in galaxies in groups - see section 5.2 for details.

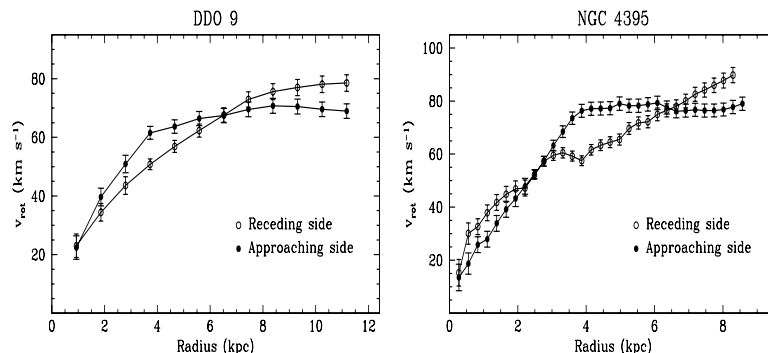


Fig. 8. The rotation curve in DDO 9 and in NGC 4395 is asymmetric on two sides of the galaxy, from Swaters et al. (1999).

A galaxy which shows spatial asymmetry would naturally show kinematical asymmetry (e.g., Jog 1997) except in the rare cases of face-on galaxies as discussed above where the galaxy can show asymmetry in the morphology but not in the kinematics. However, the papers which study lopsidedness do not always mention it. On the contrary, in the past, several papers have made a distinction between the spatial or morphological lopsidedness and kinematical lopsidedness (e.g. Swaters et al. 1999, Noordermeer, Sparke & Levine 2001) and have even claimed (Kornreich et al. 2002) that the velocity asymmetry is not always correlated with the spatial asymmetry. However, in contrast, it has been argued that the two have to be causally connected in most cases (Jog 2002), especially if the lopsidedness arises due to the disk response to a tidal encounter.

An important point to remember is that the same tracer (stars or HI) should be considered to see if a galaxy showing spatial lopsidedness is also kinematically lopsided or not, and vice versa. This is because the HI asymmetry is higher and is seen in the outer parts of the galaxy while the asymmetry in the near-IR is more concentrated in the inner regions. This criterion is not always followed (see e.g., Kornreich et al 2002). Thus the often-seen assertion in the literature that the spatial asymmetry is not correlated with kinematic asymmetry is not meaningful, when the authors compare the spatial asymmetry in the optical with the kinematical asymmetry in the HI.

### 2.3 Phase of the disk lopsidedness

The phase of the lopsided distribution provides an important clue to its physical origin, but surprisingly this has not been noted or used much in the literature. Interestingly, the phase is nearly constant with radius in the data of Rix & Zaritsky (1995), as noted by Jog (1997). This is also confirmed in the study of a larger sample of 60 galaxies by Zaritsky & Rix (1997), (Zaritsky 2005, personal communication), and also for the sample of 54 early-type galaxies studied by Rudnick & Rix (1998). A nearly constant phase with radius was later confirmed for a larger sample of 149 mostly field galaxies (Bournaud et al. 2005 b), and also for the 18 galaxies in the Eridanus group (Angiras et al. 2006). The latter case is illustrated in Fig. 9. This points to the lopsidedness as a global  $m = 1$  mode, and this idea has been used as a starting point to develop a theoretical model (Saha et al. 2007). There are a few galaxies which do show a systematic radial variation in phase, as in M51 (Rix & Rieke 1993), which therefore appear as one-armed spirals.

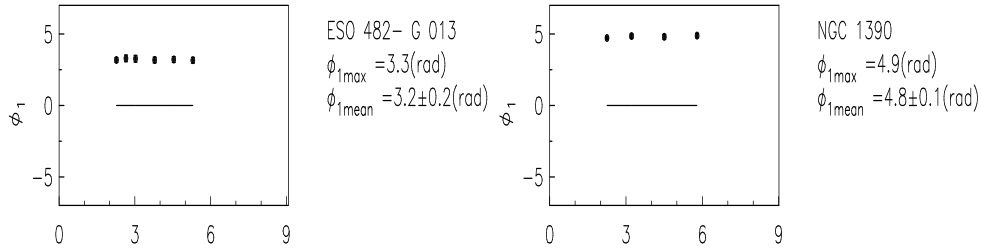


Fig. 9. The plot of the phase of the  $m=1$  Fourier component vs. radius (given in terms of the disk scalelength) for the HI surface density for two galaxies ESO 482 - G 013 and NGC 1390 in the Eridanus group of galaxies, from Angiras et al. (2006). Note that the phase is nearly constant with radius indicating a global lopsided mode.

In contrast, the central regions of mergers of galaxies, show highly fluctuating phase for the central lopsidedness (Jog & Maybhate 2006). This may indicate an unrelaxed state, which is not surprising given that the mergers represent very different systems than the individual spirals mainly discussed here.

### 2.4 Observations of off-centered nuclear disks

A certain number of galaxies are observed to have an off-centered nuclear disk, and more generally an  $m = 1$  perturbation affecting more particularly

the nuclear region. Our own Galaxy is a good example, since the molecular gas observations have revealed that the molecular nuclear disk has three quarters of its mass at positive longitude, which is obvious in the central position-velocity diagram (the parallelogram, from Bally et al 1988). The asymmetry appears to be mainly a gas phenomenon, since the off-centring is not obvious in the near-infrared images (e.g. Alard 2001, Rodriguez-Fernandez & Combes 2008). The gas is not only off-centered but also located in an inclined and warped plane (Liszt 2006, Marshall et al 2008). An  $m = 1$  perturbation is superposed on the  $m = 2$  bar instability. The most nearby giant spiral galaxy, M31, has also revealed an  $m = 1$  perturbed nuclear disk in its stellar distribution (Lauer et al 1993, Bacon et al 1994). The spatial amplitude of the perturbation is quite small, a few parsecs, and this suggests that this nuclear lopsidedness could be quite frequent in galaxies. However, it is difficult to perceive it due to a lack of resolution in more distant objects. Since M31 is the prototype of the  $m = 1$  nuclear disk, we will describe it in detail in the next section. Some other examples have been detected, like NGC 4486B in the Virgo cluster (Lauer et al 1996), but the perturbation must then be much more extended, and that phenomenon is rare.

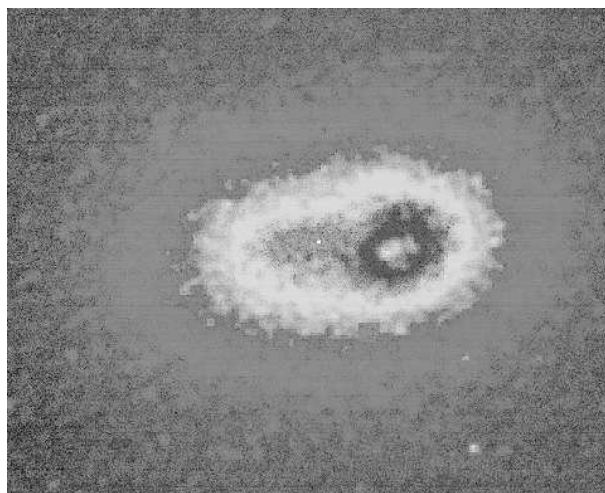


Fig. 10. HST WFPC2 V-band image of M31. The surface brightness contributed by the UV cluster coinciding with the component P2 has been clipped out. The white dot indicates the position of the black hole. ¿From Kormendy & Bender (1999).

#### 2.4.1 *The case of the M31 nuclear disk*

The first images of M31 to reveal the asymmetrical nucleus were the photographs at  $0.2''$  resolution from the Stratoscope II by Light et al (1974). They first resolved the nucleus, and measured a core radius of  $0.48''$  (1.8pc). The total size of the nucleus is 4 arcsec (15pc). They showed that the nucleus is elongated, with a low intensity extension outside the bright peak (cf Fig.

10); and they considered the possibility of a dust lane to mask the true center. Nieto et al (1986) confirmed this morphology in the near-UV and also evoked dust. Later, it was clear that dust could not be the explanation of this peculiar morphology, since the center was still offset from the bulge in the near-infrared image (Mould et al 1989). As for the kinematics, it was already remarked by Lallemand et al. (1960) that the nucleus is rotating rapidly, showing a very compact velocity curve, falling back to zero at a radius of 2 arcsec. This was confirmed by Kormendy (1988) and Dressler & Richstone (1988), who concluded to the existence of a black hole in the center of M31, of  $\sim 10^7 M_\odot$ , with the assumption of spherical symmetry. Lauer et al (1993, 1998) revealed with HST that the asymmetrical nucleus can be split into two components, like a double nucleus, with a bright peak (P1) offset by  $\sim 0.5''$  from a secondary fainter peak (P2), nearly coinciding with the bulge photometric centre, and the proposed location of the black hole (e.g. Kormendy & Bender 1999). It is well established now from HST images from the far-UV to near-IR (King et al. 1995, Davidge et al. 1997) that P1 has the same stellar population as the rest of the nucleus, and that a nearly point-like source produces a UV excess close to P2 (King et al. 1995 ).

2-D spectroscopy by Bacon et al (1994) revealed that the stellar velocity field is roughly centred on P2, but the peak in the velocity dispersion map is offset by  $\sim 0.7''$  on the anti-P1 side (Fig. 11). With HST spectroscopy the velocity dispersion peak reaches a value of  $440 \pm 70 \text{ km s}^{-1}$ . and the rotational velocity has a strong gradient (Statler et al. 1999). The black hole mass required to explain these observations ranges from 3 to  $10 \times 10^7 M_\odot$ . The position of the black hole is assumed to coincide with the centre of the UV peak, near P2, and possibly with the hard X-ray emission detected by the Chandra satellite (Garcia et al. 2000).

#### 2.4.2 *Other Off-centered nuclei*

It has been known from a long time that the nearby late-type spiral M33 has a nucleus displaced from the young population mass centroid, by as much as 500pc (de Vaucouleurs & Freeman 1970, Colin & Athanassoula 1981). This off-centreing is also associated with a more large-scale lopsidedness, and can be explained kinematically by a displacement of the bulge with respect to the disk. Such kind of off-centreing is a basic and characteristic property of late-type Magellanic galaxies. In NGC 2110, an active elliptical galaxy, Wilson & Baldwin (1985) noticed a displacement of the nucleus with respect to the mass center of 220pc, both in the light and kinematics. Many other active nuclei in elliptical galaxies have been reported off-centered, but the presence

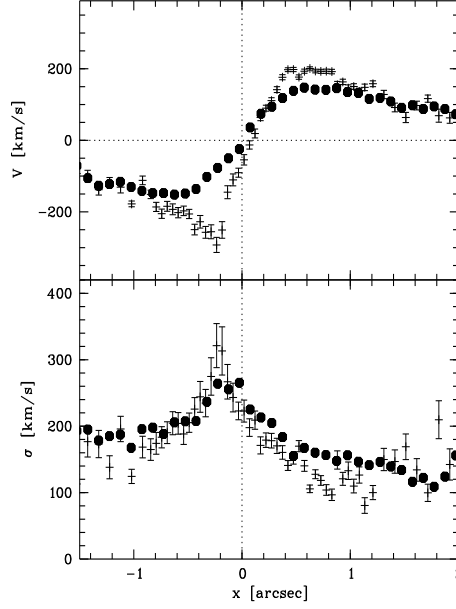


Fig. 11. Velocity profile (**top**) and velocity dispersion (**bottom**) in the nucleus of M31. The crosses are from STIS (HST) and the filled circles from OASIS (CFHT). The OASIS kinematics have been averaged over a  $0.2''$  wide slit ( $PA = 39^\circ$ ) - taken from Bacon et al. (2001).

of dust obscuration makes its reality difficult to assert (e.g. Gonzalez-Serrano & Carballo 2000, where 9 galaxies out of a sample of 72 ellipticals are off-centered).

Quite clear is the case of the double nucleus in the barred spiral M83 (Thatte et al 2000): near-infrared imaging and spectroscopy reveals, in spite of the high extinction, that the nucleus is displaced by 65pc from the barycenter of the galaxy, or that there are two independent nuclei. Molecular gas with high velocity is associated with the visible off-center nucleus, and this could be the remnant of a small galaxy accreted by M83 (Sakamoto et al 2004). In some cases what appeared to be a double nucleus could in fact be two regions of star formation in centers of mergers of galaxies as in Arp 220 (Downes & Solomon 1998).

Recently, Lauer et al (2005) studied a sample of 77 early-type galaxies with HST/WFPC2 resolution, and concluded that all galaxies with inner power-law profiles have nuclear disks, which is not the case of galaxies with cores. They found 2 galaxies with central minima, likely to have a double nucleus (cf Lauer et al 2002), and 5 galaxies having an off-centered nucleus. This perturbation also appears as a strong feature in the Fourier analysis ( $A_1$  term).

Off-centering is also frequently observed in central kinematics, where the peak of the velocity dispersion is displaced with respect to the light center (Emmellem et al 2004, Batcheldor et al 2005). Decoupled nuclear disks, and off-

centered kinematics are now clearly revealed by 2D spectroscopy.

### 3 Theoretical models for the origin of lopsidedness:

The origin and the evolution of lopsidedness are not yet well-understood and in fact not received much theoretical attention. The lopsidedness is observed in a variety of tracers and settings. It is observed in old and young stars, and in HI and H<sub>2</sub> gas, within the optical disk and far outside the optical disk as seen in the tracer HI gas, and in field galaxies and in galaxies in groups. Given all these parameters it is difficult to come up with a unique physical mechanism for the generation or the maintenance of disk lopsidedness. Indeed there could be multiple paths for it, such as tidal interactions, gas accretion, or an internal instability. The particular mechanism that dominates depends on the situation concerned as can be seen from the following discussion. Towards the end of this section (section 3.4), we give a summary of the most likely physical mechanisms for the origin of disk lopsidedness in spiral galaxies.

We also stress that the standard  $m=2$  case has been extensively studied for years both analytically as well as by N-body simulations, both in the context of central bars (e.g. Binney & Tremaine 1987, Combes 2008, Shlosman 2005) or as two-armed spiral features (Rohlf 1977, Toomre 1981). Thus the basic physics of their growth and dynamics is fairly well-understood. In contrast, the  $m=1$  feature has just begun to be studied. We discuss the physical differences between these two cases ( $m=1$  and  $2$ ), and later in Section 6 a comparison between their observed values is made.

#### 3.1 Kinematical model for the origin of lopsidedness

The simplest way to explain the observed lopsided disk distribution is to start with a set of aligned orbits and see how long these will take to get wound up, as was done by Baldwin et al. (1980), see Fig. 12. It is well-known that the differential rotation in a galactic disk would tend to smear any material feature over a few dynamical timescales. Baldwin et al. (1980) showed that on taking account of the epicyclic motion of the stars, the effective radial range over which the differential motion affects the winding up is reduced by nearly a factor of 2, and this helps in increasing the lifetime of the feature. The net winding up time  $t_{winding}$ , for a feature between two radii  $R_1$  and  $R_2$  is then given by  $t_{winding} = 2 \pi / \Delta(\Omega - \kappa)$ , where  $\Omega$  and  $\kappa$  are the angular speed of rotation and the epicyclic frequency respectively, and  $\Delta$  denotes the difference taken at these two radii. For a flat rotation curve with  $\kappa = 1.414\Omega$ , this gives  $t_{winding} = 5 [2 \pi / \Delta\Omega]$ , which is about 5 times longer than the usual winding

up time for material arms.

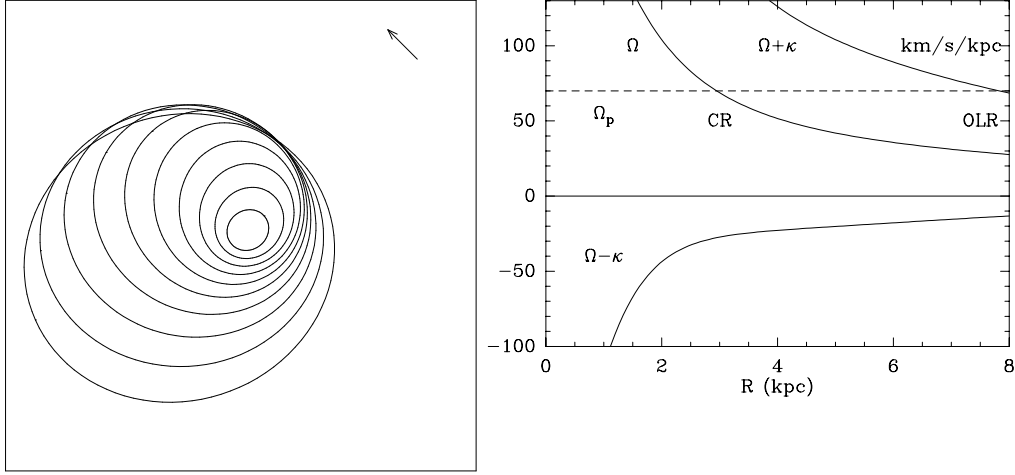


Fig. 12. *Left*: Pattern of lopsided elliptical orbits whose major axes were aligned to begin, following Baldwin et al. (1980). The orbits tend to get misaligned with time due to the differential rotation in the disk. *Right*: Frequencies  $\Omega$ ,  $\Omega - \kappa$  and  $\Omega + \kappa$  in a typical galaxy disk. In the case of a prograde mode, a possible pattern speed  $\Omega_p$  is indicated, allowing Corotation (CR) and Outer Lindblad Resonance (OLR) (taken from Combes 2000).

For the outer parts of a galaxy say at  $\sim 15$  kpc, this is  $\sim 2$  Gyr, which is a few times larger than the local dynamical timescale but is still less than the lifetime of the Galaxy. Hence they argued that the lopsidedness cannot be primordial, and must be generated repeatedly in the disk. Further, this model cannot explain why many isolated galaxies such as M101 show lopsidedness, which is the puzzle they had started out to solve.

Further work on the kinematical origin of lopsidedness due to a cooperation of orbital streams of stars near resonance was done by Earn & Lynden-Bell (1996), with similar results for its lifetime as discussed above. Apart from the short winding time, a generic problem with the kinematical model is that it is not clear what gives rise to the aligned orbits in the first place.

### 3.2 Dynamical models for the origin of lopsidedness

The set of dynamical models discussed next deal with a more physical origin for the lopsidedness. The most commonly proposed models include tidal encounters, gas accretion, instability in a counter-rotating disk, an off-centered disk in the halo, and ram pressure stripping in a cluster. Of these the most

promising are the first two, with the tidal encounters being the dominant mechanism for group galaxies. In addition to these externally triggered processes, the disk lopsidedness could also arise as a global  $m=1$  instability in self-gravitating disks.

### *3.2.1 Tidal encounters, and disk response to distorted halo*

One of the earliest ideas suggested for generating lopsidedness in a galaxy was due to a tidal encounter as applied to M101 (Beale & Davies 1969), although no details were worked out. It is easy to see that a perturbation as say due to a tidal encounter between two galaxies with an arbitrary orientation can generate a force term of type  $\cos \phi$ , which can then generate lopsidedness in the galaxy (Combes et al. 2004, see Chapter 7.1.1). The other modes will also be generated but generally  $m=1$  and 2 are observed to be the strongest (Rix & Zaritsky 1995). Also see Section 6 for a discussion the observed relative strengths of the  $m = 1$  and 2 modes.

In addition to the above direct triggering of lopsidedness as a disk response to the tidal force, it can also be generated more indirectly due to the response of the disk to the distorted halo which feels a stronger effect of the interaction (Weinberg 1995, Jog 1997, Schoenmakers et al. 1997). The details of lopsidedness thus induced will be summarised in this section. The effect can be seen as in the spatial or surface density distribution as well as in the kinematics.

A generally stronger perturbation resulting from the infall of a satellite galaxy can also result in the disk lopsidedness as shown in the N-body simulation study by Walker et al. (1996). Zaritsky & Rix (1997) further used this idea to constrain the rate of infall of satellites onto a galaxy from the fraction of galaxies showing lopsidedness and the star formation, both triggered by the satellite infall. Note that this gives an upper limit on the satellite infall rate if there are other mechanisms which also give rise to the disk lopsidedness; such as gas accretion as discussed in Section 3.2.2.

Since the dark matter halo is more extended than the disk, during a tidal encounter the halo is expected to experience a stronger tidal perturbation on general grounds. Weinberg (1995, 1998) has studied this case numerically for the specific case of the interaction between the LMC and the Galaxy. The live halo shows a strong lopsided response at the resonance points as set by the orbit of the LMC with respect to the Galaxy. The disk response to this distorted halo is shown to be much stronger than the direct lopsidedness triggered in it due to the encounter. A detailed numerical evolution of a galactic disk and the halo perturbed by an impulsive perturbation (Kornreich et al. 1998) shows that  $m=1$  can grow as a free sloshing libration but can only last for a dynamical timescale. On the other hand, a number of encounters covering a



large parameter space for the galaxy mass ratios, orbits, disk inclination were studied by numerical simulations by Bournaud et al. (2005 b). They conclude that the resulting lopsidedness can have an amplitude as high as the typical observed value  $\sim 10\%$ , and it lasts for more than ten dynamical timescales  $\sim 2$  Gyr, after which the lopsidedness drops rapidly.

### 3.2.1.a *Orbits and isophotes in a perturbed disk*

We next briefly summarise the results for the orbits, isophotes and kinematics for a disk that is perturbed by a linear lopsided perturbation potential, as say due to a distorted halo (Rix & Zaritsky (1995), Jog (1997, 2000), Schoenmakers et al (1997)) where the halo distortion could be ascribed to a tidal encounter. These equations of motion are general and are applicable irrespective of the mechanism giving rise to the external potential to which the disk responds. This simple model allows one to draw general conclusions about the strength of the perturbation potential by a comparison of results with observations as is shown next.

The details of this approach (Jog 2000) are summarised below. The dynamics of particles on closed orbits in an axisymmetric disk perturbed by a lopsided halo potential is treated. The cylindrical coordinate system  $(R, \phi)$  in the galactic disk plane is used.

The unperturbed, axisymmetric potential in the disk plane,  $\psi_0(R)$ , and the perturbation potential,  $\psi_{lop}(R)$  are defined respectively as:

$$\psi_0(R) = V_c^2 \ln R \quad (1)$$

$$\psi_{lop}(R) = V_c^2 \epsilon_{lop} \cos \phi \quad (2)$$

where  $\psi_0(R)$  represents the typical region of flat rotation, with  $V_c$  being the constant rotational velocity, as seen in a typical spiral galaxy. This is perturbed by a small, constant, non-rotating, perturbation potential with a lopsided form as given by  $\psi_{lop}(R)$ . Here  $\epsilon_{lop}$  is a small perturbation parameter, which is taken to be constant with radius for simplicity. That is, a halo with a constant lopsided distortion is assumed. This is a simple model but it still allows one to understand the resulting orbits, isophotes and the kinematics in a lopsided galaxy.

Consider a circular orbit at  $R_0$ . The coupled equations of motion for the perturbed quantities  $\delta R$  and  $\delta \phi$  are solved together using the first-order epicyclic theory. The resulting solutions for the perturbed motion are:

$$R = R_0(1 - 2\epsilon_{lop}\cos\phi) ; \quad V_R = 2V_c\epsilon_{lop}\sin\phi ; \quad V_\phi = V_c(1 + 3\epsilon_{lop}\cos\phi) \quad (3)$$

Thus, an orbit is elongated along  $\phi = 180^\circ$ , that is along the minimum of the lopsided potential, and it is shortened along the opposite direction. This result was also noted by Earn & Lynden-Bell (1996).

The loop orbits discussed here are not valid for radii much smaller than the disk scalelength (Rix & Zaritsky 1995), but this does not affect the applicability of this analysis to galactic disks because the disk lopsidedness is typically observed only at radii beyond 1.5 disk scalelengths.

The other signatures of the effect of the lopsided perturbation potential are its effect on the isophotes and the kinematics in the disk, discussed next. Since the imaging observations give information on the isophotes rather than orbits, it is necessary to also obtain the isophotal shapes in an exponential galactic disk in a lopsided potential. For an exponential disk, the above approach gives:

$$A_1 = \frac{\epsilon_{iso}}{2} \frac{R}{R_{exp}} \quad (4)$$

where  $\epsilon_{iso}$  is the ellipticity of the isophote at  $R$ , and  $R_{exp}$  is the exponential disk scale length. Note that here the radii measuring the minimum and maximum extents of an isophote are along the same axis - unlike in the standard definition of ellipticity where these two are along directions that are normal to each other. *The resulting isophotes have an egg-shaped oval appearance*, as observed say in M 101. Thus, the azimuthal asymmetry in the surface density or the fractional Fourier amplitude for  $m=1$ , as denoted by  $A_1$  manifests itself as an elongation of an isophote, and both represent the same underlying phenomenon.

The effective surface density in a self-gravitating, exponential galactic disk may be written as:

$$\mu(R, \phi) = \mu_0 \exp\left[-\frac{R}{R_{exp}}\left(1 - \frac{\epsilon_{iso}}{2}\cos\phi\right)\right] \quad (5)$$

For a particular isophote, the term in the square bracket is a constant and hence this formally defines the parametric form of an isophote. Thus the minimum radius of an isophote occurs along  $\phi = 180^\circ$  while the maximum occurs along  $\phi = 0^\circ$ ; while the opposite is true for an individual orbit. Thus the isophotes are elongated in a direction opposite to an orbit, and the elonga-

tion is along the same direction where the maximum effective surface density occurs- this will be true for any self-gravitating system (Jog 1997).

To obtain the lopsided potential in terms of the observed lopsided Fourier amplitude, the equations of perturbed motion (eq. [3]) have to be solved with the equation of continuity, and the effective surface density (eq. [5]). Now, the equation of continuity is given by:

$$\frac{\partial}{\partial R} [R\mu(R, \phi) V_R(\phi)] + \frac{\partial}{\partial \phi} [\mu(R, \phi) V_\phi(\phi)] = 0 \quad (6)$$

Solving these, and combining with eq.[4], yields the following important results (valid for  $R \geq R_{exp}$ ):

$$\epsilon_{lop} = \frac{A_1}{(2R/R_{exp}) - 1} \quad (7)$$

and,

$$\epsilon_{iso}/\epsilon_{lop} = 4(1 - \frac{R_{exp}}{2R}) \quad (8)$$

Thus, the ellipticity of isophotal contours  $\epsilon_{iso}$  is *higher by at least a factor of 4* compared to  $\epsilon_{lop}$ . Thus even a  $\sim$  few % asymmetry in the halo potential leads to a large  $\sim$  10% spatial lopsidedness in the disk. This makes the detection of lopsidedness easier, and it explains why a large fraction of spiral galaxies is observed to be lopsided.

For the typical observed values of  $A_1 \geq 0.1$  at  $R/R_{exp} = 1.5 - 2.5$  (see Section 2.2), the typical  $\epsilon_{lop} \sim 0.03$  (from eqs.[3], and [4]), or  $\sim 0.05$  in view of the negative disk response discussed next. Thus, from the observed disk lopsidedness, we obtain a value of the *halo lopsidedness*. In the limiting case of high observed  $A_1 \sim 0.3 - 0.4$ , the resulting  $\epsilon_{lop}$  is still small  $\leq 0.1$ , this is due to the high ratio of  $\epsilon_{iso}/\epsilon_{lop}$  (eq. 8). This is an interesting physical result, because it means that despite the visual asymmetry, such galaxies are dynamically robust.

The above results for orbits and isophotes are shown to be applicable for both stars and gas in the same region of the galaxy since they respond to the same lopsided potential and have comparable exponential disk scale lengths (Jog 1997). This was confirmed by a detailed comparison of the Fourier analysis of the two-dimensional HI data and the 2MASS near-IR representing stars for a few galaxies in the Eridanus group (Angiras et al. 2006) and in Ursa Major (Angiras et al. 2007). The two tracers show comparable lopsided amplitudes

(see Fig. 25). This is true even though the HI gas in these group galaxies obeys a gaussian rather than an exponential radial distribution.

In the above analysis, the phase is taken to be constant with radius and hence set equal to zero. When the phase of the potential varies with radius, the resulting isophotes show a prominent one-arm, as observed in M51 and NGC 2997.

### 3.2.1.b Kinematics in a perturbed disk

The kinematics in the disk perturbed by a lopsided potential is also strongly affected. The net rotational velocity,  $V_\phi$ , (see eq. [3]), is a maximum at  $\phi = 0^0$ , and it is a minimum along the opposite direction. This results in distinctly *non-axisymmetric rotation curves* in the two halves of a galaxy (Jog 1997), with the maximum difference between the rotational velocities  $\sim 10\%$  or 20-30  $\text{km s}^{-1}$  for the typical observed  $A_1$  values (Jog 2002). This naturally explains the observed asymmetry in rotation curves of galaxies such as M 101. The observers most often give an azimuthally averaged data, thereby the precious information on the kinematical asymmetry is lost. It is strongly recommended (see Jog 2002) that the observational papers give, when possible, a full azimuthal plot of the rotation velocity or at the very least the average taken in each hemisphere separately. The latter is done in many papers- see e.g. Begeman 1987, which can be used to deduce the kinematical asymmetry in galaxies. Such asymmetry has also been studied by Swaters et al. (1999) from their kinematical data in HI on DDO 9 and NGC 4395. They show that the rotation curve rises more steeply in one half of the galaxy than in the other.

The asymmetry in the velocity fields resulting from the disk response to a lopsided halo perturbation has also been studied by Schoenmakers (1999). The results obtained are applied to analyze the kinematical data from a few spiral galaxies (Schoenmakers et al. 1997, Swaters et al. 1999). Schoenmakers et al (1997) show that the Fourier amplitudes  $m + 1$  and  $m - 1$  of the velocity field are affected when the perturbation potential of type  $m$  is considered. By comparing the observed values for  $m = 2$  with the calculated values they obtain an upper limit (uncertain up to the sine of the inclination angle) for the lopsided perturbation potential.

The approach described in this section assumes a simplified perturbation lopsided potential with a constant amplitude, also only closed orbits are considered for simplicity. The orbits would change slightly and would not be closed if the random motion of the particles is taken into account. However, this does not affect the isophotal shapes - see Rix & Zaritsky (1995).

### 3.2.1.c Radius for the onset of disk lopsidedness

The lopsided distribution in a disk cannot self-support itself because the potential corresponding to it opposes the perturbation potential, as discussed next. The effective disk surface density or the disk density response is shown to be a maximum along  $\phi = 0^0$ , that is along the maximum of the lopsided potential (Jog 1997), see eq.(5) above. This has interesting and subtle dynamical consequences (Jog 1999). This can be seen from the self-gravitational potential corresponding to the non-axisymmetric disk response, which is obtained by inversion of Poisson equation for a thin disk using the Henkel transforms of the potential-density pairs. This response potential is shown to oppose the imposed lopsided potential. This may seem counter-intuitive but it arises due to the self-gravity of the disk. Thus in the inner parts of the disk, the disk resists any imposed perturbation potential.

A self-consistent calculation shows that the net lopsided distribution in the disk is only important beyond 1.8 disk scale lengths and its magnitude increases with radius. This indicates the increasing dynamical importance of halo over disk at large radii. The negative disk response decreases the imposed lopsided potential by a factor of  $\sim 0.5 - 0.7$  (Jog 2000). The above radial dependence agrees well with the onset of lopsidedness as seen in the near-IR observations of Rix & Zaritsky (1995). On taking account of this effect, a given observed lopsided amplitude corresponds to the deduced perturbation potential to be higher by a factor of  $\sim 1.3 - 1.4$ .

The radius of onset of lopsidedness and the reduction in the imposed potential depend on the form of the perturbation potential which was taken to be constant for simplicity in Jog (1999). A more realistic case with a radially varying perturbation potential as in a tidal encounter with amplitude decreasing at low radii, will result in the highest decrease at lowest radii (Pranav & Jog 2008). In this case the actual value of reduction will decide the radius beyond which net disk lopsidedness is seen.

This idea of negative disk response is a general result and is applicable for any gravitating system which is perturbed by an external mechanism. Although it is shown here for a  $\cos\phi$  perturbation resulting from a tidal perturbation, it is applicable for any linear perturbation of the system. A similar study for the onset of warps (which can be represented by an  $m=1$  mode along the vertical direction) has been done (Saha & Jog 2006). This shows the onset of warps from a radius of 4-5 disk scalelengths, in good agreement with observations (Briggs 1990). The disk self-gravity is more important along the z-direction for a thin disk and hence the disk is able to resist vertical distortion till a larger radius than the planar distortion.

### 3.2.1.d Comparison of $A_1$ vs. tidal parameter

Since tidal encounters (e.g. Beale & Davis 1969, Weinberg 1995) and satellite accretion (Zaritsky & Rix 1997) have often been suggested as the mechanism for the origin of the disk lopsidedness, it is instructive to check how the observed amplitude  $A_1$  for lopsidedness varies with the tidal parameter  $T_p$  as was done by Bournaud et al. (2005 b). The tidal parameter  $T_p$  was calculated in each case as:

$$T_p = \log \Sigma_i \left[ \left( \frac{M_i}{M_0} \right) \left( \frac{R_0}{D_i} \right)^3 \right] \quad (9)$$

where the sum is computed over the companions for a galaxy of target mass  $M_0$  and radius  $R_0$  and  $M_i$  is the mass of the companion at a projected distance  $D_i$  on the sky. The summation is over neighbours within 2 degrees on the sky and within  $500 \text{ km s}^{-1}$  velocity range of the test galaxy.

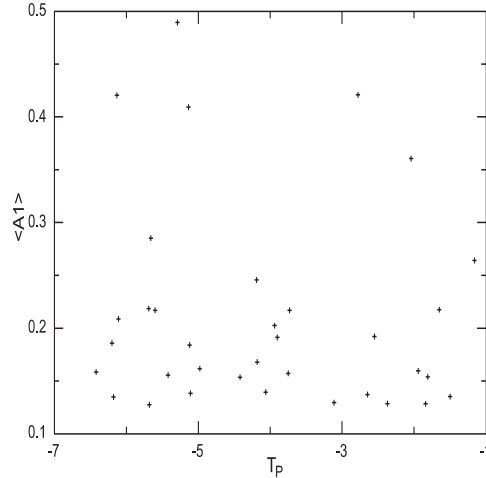


Fig. 13. Plot of  $A_1$  vs. tidal parameter for the 35 strongly lopsided galaxies in the OSU sample (taken from Bournaud et al. 2005 b). There is no correlation between these quantities, in particular the isolated galaxies with high  $A_1$  (top l.h.s. corner of this plot) cannot be explained by a recent tidal interaction.

The result is plotted in Figure 13, for the 35 most lopsided galaxies which are at an inclination of  $< 70^\circ$ . Surprisingly, this does not show a correlation between the lopsided amplitude and the strength of the tidal parameter. In particular it is hard to explain the galaxies with high  $A_1$  and low tidal parameter (in the top l.h.s. of this figure) in the tidal picture. On the other hand, this still does not rule out tidal encounters as the origin for lopsidedness if it is long-lived, or if it arises due to a satellite merger (Walker et al 1996, Bournaud et al. 2005 b).

In order to check the typical values of lopsided amplitudes generated in tidal encounters and satellite accretion, N-body simulations for a number of encounters and satellite mergers were studied. They included the tidal encounters between nearly equal-mass galaxies (up to the ratio of 4:1) and mergers of small-mass galaxies (in the ratio of 5:1-20:1) (Bournaud et al. 2005 b). It was found that tidal interactions can indeed generate a fairly large amplitude similar to or higher than the average value of  $\sim 0.1$ . However, the amplitude then drops rapidly and hence can be seen only for  $< 2$  Gyr. A typical example of an encounter between a 2:1 mass ratio is shown in Figure 14. Thus tidal encounters cannot explain the high amplitude of lopsidedness seen in several isolated galaxies such as NGC 1637, although it could arise due to a recent satellite accretion. While a satellite accretion of mass ratio 7:1-10:1 can result in a strong lopsidedness, it can also thicken the disk more than is observed (Bournaud, Combes, & Jog 2004, Bournaud et al. 2005 a). The thickening of disks can set a limit on the rate of satellite mergers (Toth & Ostriker 1992). It needs to be checked if a small-mass satellite falling onto a galactic disk can generate the right amplitude distribution of lopsidedness without thickening the disk, and further if there exist satellites in sufficient numbers to fall in at a steady rate to repeatedly generate lopsidedness as required by the observed high fraction of lopsided galaxies.

The mechanism for origin of lopsidedness involving a tidal encounter has been explored by Mapelli et al. (2008) in the context of NGC 891. They show that the lopsidedness seen in the atomic hydrogen gas in NGC 891 is due to the fly-by encounter with its neighbour UGC 1807. They argue that this is a preferred mechanism over gas accretion from cosmological filaments or that due to ram pressure from the intergalactic medium.

Further, a number of statistical features for the field galaxies show that a tidal encounter cannot be the primary mechanism for the origin of the disk lopsidedness- for example, the lopsidedness is higher for late-type galaxies whereas tidal encounters and mergers would tend to lead to the secular evolution of a galaxy towards early-type galaxies. Thus if tidal interactions were the primary mechanism for generating lopsidedness, then the early-type galaxies should show a higher amplitude of lopsidedness. This is opposite to what is seen in the field galaxies (Bournaud et al. 2005 b). Thus other mechanisms such as gas accretion (Section 3.2.2) could be important in generating the lopsidedness in field galaxies.

In the group galaxies, on the other hand, the tidal interactions being more frequent, play a dominant role in generating lopsidedness. This is evident from the fact that the early-type galaxies show higher lopsided amplitudes as seen in the Eridanus group galaxies (Angiras et al. 2006) and less strongly in

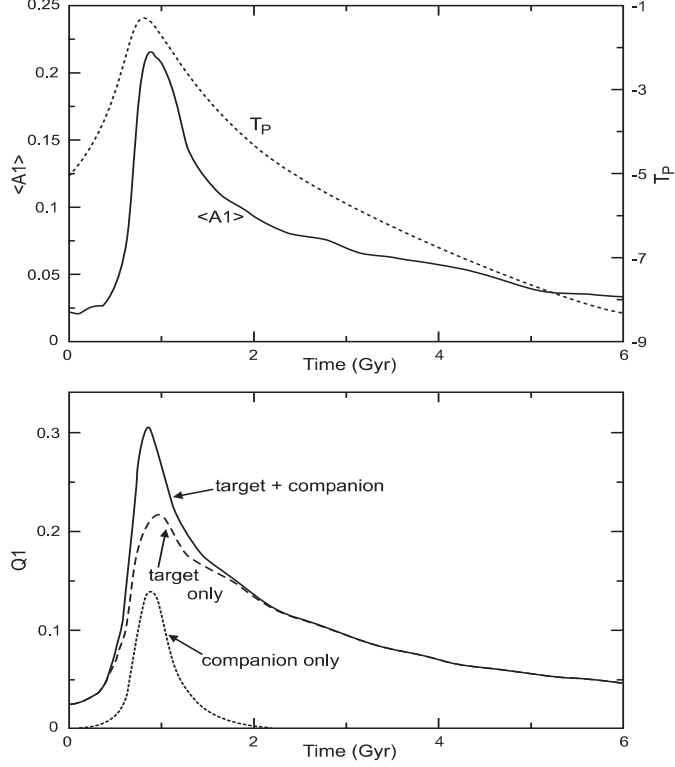


Fig. 14. Plot of  $A_1$  vs. time in the middle radial range of 1.5-2.5 disk scalelengths, generated in a distant interaction between galaxies of mass ratio 2:1 (taken from Bournaud et al. 2005 b). The peak value of  $A_1$  is large  $\sim 0.2$ , higher than the average value seen in the OSU field galaxies sample, but it drops rapidly to 0.05 in a few Gyr. The lower panel shows the same in terms of  $Q_1$ , the cumulative potential from the disk.

the Ursa Major group of galaxies (Angiras et al. 2007). The details are given in Section 5.

### 3.2.2 Gas Accretion, and other mechanisms

The intergalactic gas accretion was proposed as a qualitative idea to explain the  $m=1$  asymmetry in NGC 4254 by Phookun et al.(1993). They proposed that the lopsidedness could arise due to the subsequent swing amplification in stars and gas (as in Jog 1992). An extensive study of origin of lopsidedness via N-body simulations (Bournaud et al. 2005 b) shows that while tidal encounters can explain the observed amplitudes of disk lopsidedness, these cannot explain the various observed statistical properties such as the correlation between  $A_1$  and  $A_2$ , and the higher lopsidedness seen for the late-type field galaxies. In order to do this, one needs to take account of gas accretion from outside the galaxy.

There is growing evidence that galaxies steadily accrete gas from the external



regions, as seen from the cosmological models (Semelin & Combes 2005), and also observed in nearby galaxies (Sancisi et al. 2008). Thus it is natural to see how this affects the mass distribution in a disk. While the details of gas infall are not yet well-understood, it is plausible that a galaxy may undergo an asymmetric gas infall on the two sides from say two different external filaments. An application of this idea showed that the gas infall and the resulting star formation can well reproduce the striking asymmetry observed in NGC 1367 (Bournaud et al. 2005 b), see Fig. 15 here.

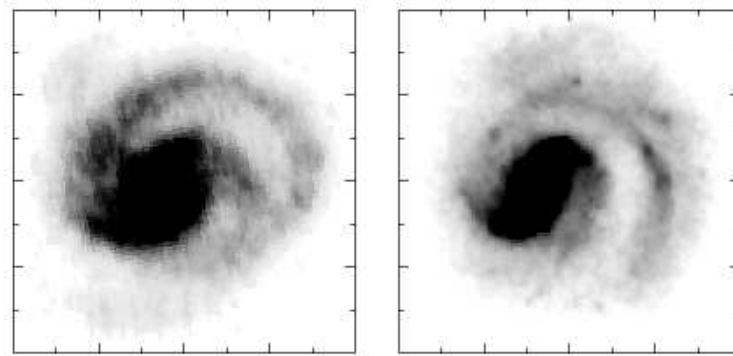


Fig. 15. NGC data - near-IR data (left panel), and the same from N-body simulations with gas accretion in two streamers at a rate so as to double the mass of the galaxy in a Hubble time (right panel), taken from Bournaud et al. (2005 b).

A word of caution is that if gas accretion is the mechanism for generation of lopsidedness, one would expect to see asymmetry in the gas velocity fields whereas these are smoothly continuous as pointed out by Baldwin et al. (1980). In the case of galaxies in groups, in any case, the tidal interactions may play a dominant role, see Section 5.2 for the details.

Other physical models have also been developed in the literature but these are probably not as widely applicable due to the specific parameters or conditions chosen, as discussed below. This includes a proposed model where the growth of  $m=1$  is treated as an instability in a self-gravitating disk (Lovelace et al 1999). This results in strongly unstable eccentric motions but only within the central disk scalelength. Here a linear analysis is used to treat slowly growing mode, and the pattern speed could be either positive or negative. In another model where the disk is off-centered with respect to the halo up to a maximum distance of the core radius (Levine & Sparke 1999) also shows lopsidedness. However, it is seen only in the inner regions within the core radius of the halo where the halo density and hence the rotation speed is constant. Both these papers do not yield higher lopsidedness in the outer parts, and this result contradicts the observations which preferentially show lopsidedness in the outer parts of a galaxy. The kinematical and morphological asymmetries resulting from the latter model are shown to be not always correlated (Noordermeer et

al. 2001). This is somewhat unexpected - since on general physical grounds the two would be expected to be related causally (see Section 2.2). In any case, the restricted set of initial conditions required for this model makes it applicable only to a few galaxies such as the dwarf galaxies.

A self-consistent model for  $m=1$  in a self-gravitating disk has been proposed by Syer & Tremaine (1996) in the so-called razor-thin disks. However, the density response due to an imposed perturbation opposes the perturbing force (see Jog 1999) and hence the disk asymmetry cannot result from the orbital asymmetry as was also argued by Kuijken (1993) and Earn & Lynden-Bell (1996). Moreover, the model by Syer & Tremaine (1996) gives the density response to be maximum along the perturbed force, which is in contrast to the result by Rix & Zaritsky (1995), and Jog (1999).

### 3.2.3 *Lopsidedness as an instability*

An obvious possible explanation for the origin of the lopsided mode is that it arises due to gravitational instability in the disk. For example, this was proposed and studied for the gas by Junqueira & Combes (1996). A similar model for the disk in a dark matter halo perturbed by a satellite was studied by Chan & Junqueira (2003), however these models generate lopsidedness only in the inner regions in contrast to the observed trends. An internal mechanism based on the non-linear coupling between  $m=2$  (bars or spiral arms) and  $m=3$  and  $m=1$  has been proposed by Masset & Tagger (1997) which gives rise to the excitation of  $m=1$  modes in the central regions.

Lopsided instabilities have been shown to develop in counter-rotating stellar disks which have a high fraction of retrograde orbits (Hozumi & Fujiwara 1989, Sellwood & Valluri 1997, Comins et al 1997, Dury et al 2008). Galaxies where the gas participates to the counter-rotation are quite often observed to develop  $m = 1$  perturbations (e.g. Garcia-Burillo et al 2000, 2003). However, since counter-rotation is rarely seen in stellar disks (Kuijken, Fisher, & Merrifield 1996, Kannappan & Fabricant 2001, McDermid et al 2006), this cannot be the primary mechanism for the generation of lopsidedness in disks.

In a recent work, the self-gravity of a slowly-rotating global  $m=1$  mode has been shown to lead to a long-lasting lopsided mode in a purely exponential disk as in a spiral galaxy (Saha, Combes, & Jog 2007). This model was motivated by the fact that the observations show that the lopsidedness has a constant phase with radius which indicates a global mode. Further, it was noted that  $m=1$  is unique in that the centre of mass of the disturbed galaxy is shifted away from the original centre of mass and thus acts as a restoring force on the latter. Thus the system can self-support the  $m=1$  mode for a long time especially when one takes account of the self-gravity of the global mode.

Using the linearized fluid equations and the softened self-gravity of the perturbation, a self-consistent quadratic eigenvalue equation is derived for the lopsided perturbation in an exponential galactic disk and solved. Fig. 16 shows the resulting isodensity contours, clearly the centres of isocontours are progressively more disturbed in the outer parts.

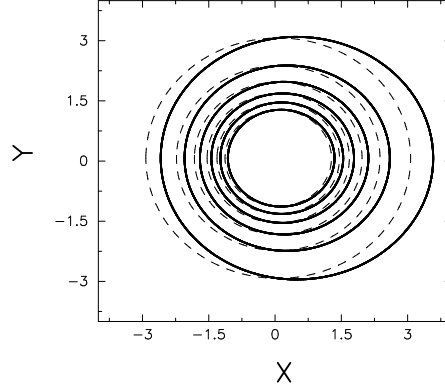


Fig. 16. Contours of constant surface density for a global  $m=1$  mode, taken from Saha et al. (2007). Here the  $x$  and  $y$  axes are given in units of the disk scalelength. The maximum surface density occurs at  $(0,0)$ . The outer contours show a progressive deviation from the undisturbed circular distribution, indicating a more lopsided distribution in the outer parts- as observed.

The self-gravity of the mode results in a significant reduction in the differential precession, by a factor of  $\sim 10$  compared to the free precession. This leads to persistent  $m=1$  modes, as shown in Fig. 17.

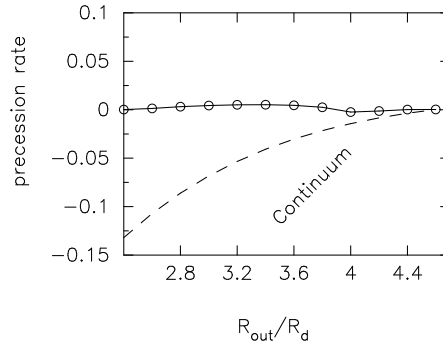


Fig. 17. The precession rate for the global lopsided mode vs. the size of the disk in units of the disk scalelength in a galactic disk (shown as the line with circles) is very low, thus the mode is long-lived. The dashed line denotes the free precession  $(\kappa - \Omega)$ . This is taken from Saha et al. (2007).

N-body simulations are performed to test the growth of lopsidedness in a pure stellar disk, which confirm these results (see Fig. 18). Both approaches are

compared and interpreted in terms of slowly growing instabilities on timescales of  $\sim$  a few Gyr, with almost zero pattern speed.

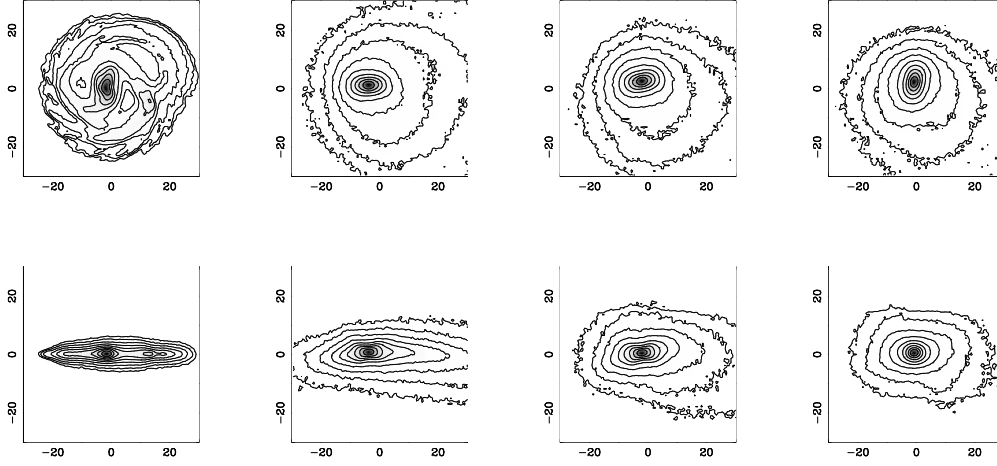


Fig. 18. The isodensity contours in a purely stellar exponential galactic disk, given in a logarithmic scale of the surface density of the stellar disk, face-on (top panel) and edge-on (lower panel) views at four different epochs:  $T = 0, 4.8, 9.6, 14.4$  Gyr, from left to right, taken from Saha et al. (2007). The global lopsided mode is long-lived and lasts for  $\sim 14$  Gyr.

Though this is a somewhat idealized approach, it is precisely this that has allowed the authors to focus on the basic dynamics of the excitation and growth of  $m=1$  modes. For example, here the only important input parameters are the softening and the Toomre  $Q$  parameter. A smaller value of Toomre  $Q$  results in a fast initial growth of the mode but later as the  $Q$  increases due to the heating in the system, the mode is self-regulated and has a nearly constant amplitude  $A_1$  that is long-lived. The softening acts as an indicator of the coherence in the mode, and a higher value results in a faster growth rate of the modes. These global modes are precessing remarkably slowly, and therefore are relatively long-lived. Numerical analysis of the eigen modes of a cold thin disk shows that, if treated as modes of zero pattern speed, warps and lopsidedness are fundamentally similar in nature (Saha 2008).

Such small pattern speed is also in agreement with the work of Ideta (2002) who showed that the rotating  $m=1$  mode in a live halo would be damped very rapidly by the density wake induced in the halo, see Fig. 19. Hence he argued that the  $m=1$  modes must be non-rotating at a rate smaller than  $1 \text{ km s}^{-1} \text{ kpc}^{-1}$ . This would give the damping time to be comparable to the Hubble time, which can explain the high frequency of lopsidedness seen in spiral galaxies.

In a recent paper Dury et al. (2008) have studied a galactic disk in an inert

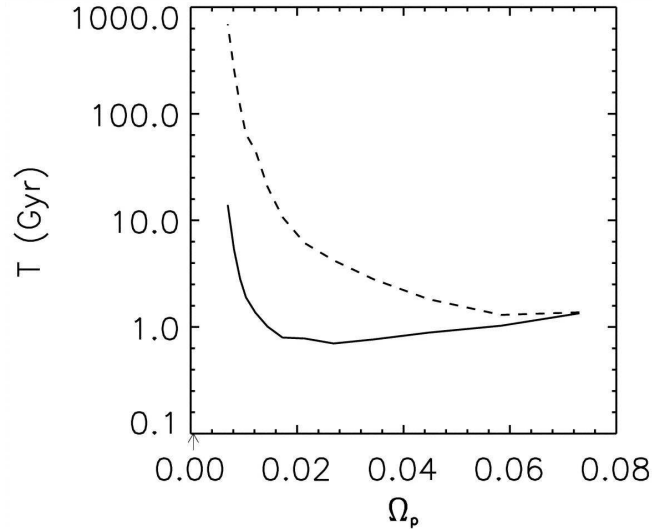


Fig. 19. The damping time of the lopsided mode vs. the pattern speed, for a self-gravitating case (solid line) and without self-gravity (dashed line) respectively, taken from Ideta (2002). Damping times  $\sim$  Hubble time imply a very low pattern speed of the lopsided mode.

halo by N-body simulations and argued that that a rotating  $m=1$  mode can occur as a result of the swing amplification (Toomre 1981).

#### 3.2.4 *Effect of inclusion of rotation and a live halo*

The work by Saha et al. (2007) shows that a gravitating disk is susceptible to the growth of  $m=1$  modes, irrespective of the origin of these modes. These could be triggered as a response to a distorted halo, or by gas accretion. We caution, however, that Saha et al. (2007) treat a simple, specialized case of slow rotating modes in a pure exponential disk. A more realistic treatment should include a live or a responsive halo in addition to the disk. Here more parameters enter the picture such as the relative mass of the halo and the disk, and ratio of the core radius of the halo to the disk scalelength etc. The inclusion of a live halo is expected to further support the persistent  $m=1$  modes, in analogy with what was shown for bars by Athanassoula (2002) and for a general, local non-axisymmetric feature by Fuchs (2004). In contrast, other papers suggest that a responsive halo tends to damp a feature in the disk by the wake created in the halo. This was shown for disk lopsidedness ( $m=1$  in the plane) by Ideta (2002), and shown in the case of warps treated as an  $m=1$  mode normal to the galactic plane (Nelson & Tremaine 1995). This issue needs to be clarified by further dynamical studies of a global  $m=1$  mode of an arbitrary pattern speed in a galactic disk. This study should include a live halo, and have a high resolution (since poor resolution may smoothen the response and give a spuriously long-lasting mode), with the aim to check the lifetime of such a mode.

A lopsided mode in a collisionless spherical dark matter halo is shown to be long-lasting or slowly damped compared to the dynamical timescales (Weinberg 1994, Vesperini & Weinberg 2000). However it is not clear if this is due to the fact that the halo is supported by random motion and hence a perturbation in it is long-lived. On the other hand, in a spiral galaxy, the presence of differential rotation puts a limit on any material feature due to the precession rate. In contrast, the numerical simulations of perturbations triggered in a galaxy with live halo, due to the tidal encounter of nearly equal-mass galaxies (up to the ratio of 4:1) and mergers of small-mass galaxies (in the ratio of 5:1-20:1) show that the lopsidedness thus generated, although long-lived compared to the dynamical timescales, does not last beyond  $\sim 2$  Gyr (Bournaud et al. 2005 b). The crucial factor that decides the lifetime of the lopsided mode could be its pattern speed, with the small speed cases lasting for a long-time close to the Hubble time (Ideta 2002, Saha et al. 2007). The off-centering of the mass distribution is less pronounced in the case of high rotation speed. This could lead to a short lifetime of the  $m=1$  mode as pointed out by Ideta (2002). In this case the restoring term in the equations of motion (Saha et al. 2007, eq. 18) is less pronounced and hence the  $m=1$  mode lasts for a shorter time. Alternatively, it could be that the wake generated in a halo could be larger for a higher pattern speed, and hence the halo tends to dampen such modes. This may be the reason why the lopsidedness generated in a disk with a live halo due to a tidal encounter or a minor merger (Bournaud et al. 2005 b) lasts for  $< 2$  Gyr.

While slow  $m=1$  modes are shown to be long-lived, the uniqueness of this solution is still not established, or that this is what explains the observed lopsidedness. Also it is not clear what would excite such slow modes. The generating mechanism may have a strong bearing on the resulting pattern speed: a tidal encounter is expected to result in lopsidedness with a high pattern speed  $\sim$  the relative velocity over the impact parameter as argued by Ideta (2002). Gas accretion, on the other hand, may not easily give a global  $m=1$  mode, while observations show the mode to be global. Further numerical simulations should check if a satellite accretion can give rise to a slow, global mode. An actual measurement of the pattern speed of the lopsided mode in a real galaxy will help settle this issue, and we urge observers to take up this important measurement.

### *3.3 Comparison between origin of $m=1$ and $m=2$ ; stars and gas*

As discussed at the beginning of Section 3, the  $m = 2$  case is fairly well-understood, while the  $m=1$  case has only begun to get attention from theorists. There are several differences in the dynamics and evolution of the two features, and also as applied to stars or gas. First, the presence of dark matter

halo is likely to have a substantial role to play in the origin and evolution of lopsidedness in a disk. This is especially true in the outer parts of a disk since the disk lopsidedness is observed to increase with the radial distance where the halo is more important. In the inner regions of a galaxy, on the other hand, the inclusion of the bulge is likely to play an important role in stabilizing the  $m=1$  mode (de Oliveira & Combes 2008).

Further, the  $m=1$  mode generally has no ILR (Inner Lindblad Resonance, e.g., Block et al. 1994) hence its evolution differs from that of  $m=2$ . The  $m=1$  mode does not get damped easily due to the angular momentum transport occurring at the resonance points as in the case of  $m=2$  (Lynden-Bell & Kalnajs 1972). In case of  $m=2$  this causes an absorption of the wave at the ILR and thus a break in the feedback loop. But in absence of an ILR for  $m=1$ , this break does not arise and this helps in sustaining the global  $m=1$  mode for a long time. In this picture, the gas being cold behaves in a different way. The absorption at the resonance point is only partial for gas and hence even  $m=2$  can be sustained in gas despite the presence of an ILR. This helps support the generation of  $m=2$  and higher order modes in the presence of gas.

### 3.4 *A summary of the various mechanisms*

Of the various mechanisms proposed so far, the most promising ones, as judged by the resulting agreement with the observations, are those involving tidal encounters and gas accretion.

An  $m=1$  perturbation in a disk leads to a shift in the centre of mass in the disk, and this then acts as an indirect force on the original centre of the disk. The disk is thus shown to naturally support an  $m=1$  mode, and as pointed out above, this is a characteristic property valid only of a lopsided mode. This basic physics is sometimes clouded over because of the additional effects introduced due to the inclusion of the dark matter halo, the bulge, and the gas as in a real galaxy. Further, depending on whether the halo is live or rigid, and whether it is pinned or not, and whether the pattern is rotating or stationary can lead to additional complexities. Also, other features like the wandering of the centre (Miller & Smith 1992) may introduce an  $m=1$  mode. In short, there seem many paths to get  $m=1$  in a galaxy, and therefore it is important to identify which is the most applicable one in a real galaxy.

### *Long-term maintenance of disk lopsidedness*

It has been realized from the beginning that the lopsided modes should be fairly long-lived (e.g., Baldwin et al. 1980) or excited frequently. This is needed in order to explain the high fraction of galaxies showing lopsidedness, and also the strong lopsidedness seen in isolated galaxies like M101. It has been noted

that since  $m=1$  does not have an ILR, it should be the preferred mode in the galactic disk (Section 3.3). This, however, does not say anything directly about its lifetime. The persistence of lopsided mode is still an open question, as shown by the discussion below.

While tidal encounters can generate the right lopsided amplitudes, these are not correlated with the strength of a tidal encounter (Bournaud et al. 2005 b), or with the presence of nearby neighbors (Wilcots & Prescott 2004). This could be explained if the disk lopsidedness once generated either directly in the disk, or as a response to a long-lived halo distortion, were long-lived, so that there is no clear correlation with a tidal encounter. N-body simulations with a live halo show the resulting  $m=1$  modes in the disk to last for  $\sim 2 - 3$  Gyr, which is much smaller than the Hubble time, thus these need to be triggered again. A tidal encounter will typically generate a fast mode which is expected to be not long-lived (see the discussion in Section 3.2.3).

While the satellite accretion of mass ratio 7:1-10:1 can result in a strong lopsidedness, it can also thicken the disk more than is observed (Bournaud et al. 2004). Also, it has a short lifetime of  $< 2$  Gyr (Bournaud et al. 2005 b). It further needs to be checked if a smaller-mass satellite falling onto a galactic disk can generate the right amplitude distribution of lopsidedness without thickening the disk, and if there are adequate number of such satellites that can fall in at a steady rate.

The pattern speed is expected to have a significant effect in determining the lifetime of a lopsided mode with a slow pattern being long-lived. It is not clear if a live halo will help or hinder the long-term sustenance of an  $m=1$  mode, as discussed in Section 3.2.3.

Future work needs to study the long-term maintenance of  $m=1$  modes when generated by accretion of a low-mass satellite. A similar study needs to be done for the case of gas accretion and to see if the latter gives a global mode. The observations of group galaxies with their generally stronger and frequent triggering of lopsidedness (see Section 5) can act as a constraint on any generating mechanism proposed for the field galaxies.

## 4 Lopsidedness in the central region

### 4.1 Stability of central nuclear disks

It is now well established that all galaxies with bulges or spheroids host a massive central black hole (Gebhardt et al. 2000). The central region, or nu-



clear disk, in galaxies therefore have a gravitational potential very close to the Keplerian. Some similarities exist with proto-planetary systems (Rauch & Tremaine 1996), or with the formation of new stars through accretion disks (Adams et al. 1989, Alexander et al. 2007). The nearly Keplerian potential, with the angular velocity  $\Omega \sim r^{-3/2}$  favors eccentric orbits and  $m = 1$  modes, instead of  $\Omega \sim r^{-1}$  of galactic disks which favor  $m = 2$  perturbations.

Nearly keplerian disks have the particular property that the orbit precession rate is almost zero ( $\Omega \sim \kappa$ ). If the apsides are aligned at a given time, they will stay so in a  $\Omega_p \sim 0$  mode. The self-gravity of the disk makes  $\kappa > \Omega$ , and the orbits differentially precess at a rate  $(\Omega - \kappa) < 0$ . However, if the disk self-gravity is not large, a small density perturbation could be sufficient to counteract the small differential precession. Goldreich & Tremaine (1979) showed that in the case of Uranian rings, the self-gravity could provide the slight impulse to equalize the precession rates, and align the apsides. Two kinds of waves could propagate in such disks- slow stable modes, and unstable rapid waves, growing on a dynamical time-scale.

The density wave theory (e. g., Lin & Shu 1964) predicts that in a self-gravitating stellar disk, global spiral modes can develop only between the radial range delimited by the Lindblad resonances, i.e. for  $m^2(\Omega - \Omega_p)^2 < \kappa^2$ . Only in gaseous disks, where the pressure forces dominate, acoustic waves can propagate outside this range. Considering the  $m = 1$  waves, for a pure keplerian potential (neglecting the self-gravity of the disk),  $\Omega = \kappa$ , and the perturbations are neutral. If there is some self-gravity in the disk, then  $(\Omega - \kappa) < 0$ , there is only an outer Lindblad resonance and a corotation, but no inner resonance (for prograde modes with  $\Omega_p > 0$ ), and therefore the radial range for the development of  $m = 1$  perturbations is quite large.

The study of WKB modes in a non self-gravitating gaseous disk, with truncation radii at the inner and outer boundary, was first done by Kato (1983), who found a region of trapped one-arm waves, with quite low pattern frequency, much lower than the orbital frequency. Adams et al (1989) considered the influence of self-gravity, in order to apply to young stellar objects, which can have accretion disks with masses of the same order as the central stellar mass. The self-gravity of such a disk is sufficient to modify the precession rate of nearly keplerian orbits ( $\Omega - \kappa$ ) to a common and coherent value. They found a pattern speed which is of the same order as the angular velocity in the disk, and the unstable waves develop with a growth time comparable to the dynamical time-scale. The special shape of modes is shown in Fig. 20.

Crucial to the development of the perturbations, a special characteristic of the  $m = 1$  mode is to shift the gravity center of the system from the dominant central mass (the black hole for instance), also see Section 3.2.3. In the

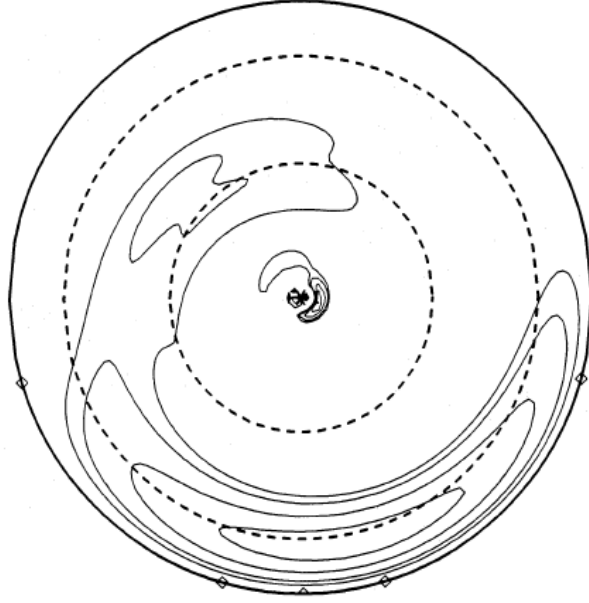


Fig. 20. Isodensity contours for the lowest order  $m = 1$  mode, in a disk of mass equal to the central point mass. Note the shape in alternating “bananas” instead of a continuous one-arm spiral. The dashed lines show the locations of the corotation and the outer Lindblad resonance. From Adams et al. (1989).

reference frame of the black hole, this implies the introduction of an inertial force, which by reference to celestial mechanics, is called the indirect term. This term is the mediator of angular momentum exchange between the disk inside and outside corotation and the central mass. The coupling with the outer Lindblad resonance provides the amplification that is usually provided by the corotation in  $m = 2$  modes. A feedback cycle has been proposed by Shu et al (1990), and called SLING (Stimulation by the Long-range Interaction of Newtonian Gravity). The modes depend strongly on the outer disk boundary conditions, since a reflection of short waves is assumed there, in the 4-waves feedback cycle. This cycle is only possible with a gaseous component, since the short waves are not absorbed at the resonance but cross the OLR (Outer Lindblad Resonance).

#### 4.1.1 *Slow stable modes, damping slowly*

Another possibility to explain central lopsidedness is to exploit the slow modes, that are stable, but can be long-lived, excited by some external mechanism, such as the accretion of a globular cluster or a giant molecular cloud. The precession rate of eccentric orbits is  $\Omega - \kappa = 0$  in the potential of a point mass  $M_{BH}$ , and slightly negative in the presence of a small disk of mass  $M_d$ , lighter than the central point mass, with amplitude varying as  $(M_d/\sqrt{M_{BH}})$  or

$\propto (M_d/M_{\text{BH}})\Omega$ . If self-gravity has a large enough role, and in particular, if the disk is cold enough and its Jeans length smaller than the disk radius,  $m = 1$  density waves can propagate; their dispersion relation has been studied in the tight-winding limit or WKB approximation (Lee & Goodman 1999, Tremaine 2001). In the linear approximation, the pattern speed for the wavelength  $\lambda = 2\pi/k$  is in first approximation for  $(M_d/M_{\text{BH}}) \ll 1$ , as given by:

$$\Omega_p = \Omega - \kappa + \frac{\pi G \Sigma_d |k|}{\Omega} F\left(\frac{k^2 c^2}{\Omega^2}\right) \quad (10)$$

where  $\Sigma_d$  is the surface density of the disk, and  $F$  the usual reduction factor that takes into account the velocity dispersion  $c$  of the stellar disk, and its corresponding velocity distribution (e.g., Tremaine 2001). The pattern speed then remains of the order of  $(M_d/M_{\text{BH}})\Omega$ , for a sufficiently cold disk, and is much smaller than the orbital frequency. These slow waves exist whenever the thin-disk Jeans length  $\lambda_J = c^2/G\Sigma_d$  is lower than  $4r$ , while the Toomre parameter  $Q$  is less relevant (Lee & Goodman 1999).

The study by Tremaine (2001) shows that disks orbiting a central mass support slow  $m = 1$  modes, which are all stable. Their frequencies are proportional to the strength of collective effects, which is either self-gravity, or velocity dispersion (or pressure in fluid disks). The latter phenomenon can be simulated with softened gravity. There are then two kinds of slow modes: the g-modes (where self-gravity is dominating, and softening is unimportant), which are long waves, with  $kr \ll 1$ , with negative frequency  $\omega < 0$ ; and the p-modes, which depend on the softening  $b$ , which can have both short and long waves ( $kr \sim b$ ), and with positive frequency  $\omega > 0$ ; as the softening increases, the amplitude of the mode decreases, as well as  $\omega$ .

In numerical N-body simulations of nuclear stellar disks, Jacobs & Sellwood (2001) have reported the presence of a slowly decaying prograde  $m = 1$  mode in annular disks around a slightly softened point mass, but only for disk masses less than 10% of the central mass concentration. This confirms the existence of a persistent slow mode, with positive  $\omega$  increasing with the mass of the disk, and decreasing with the amplitude of the perturbation.

Touma (2002) has computed the normal modes of a series of N rings in a thin disk, through linearized dynamics, and using the Laplace-Lagrange secular theory of planetary motions (valid for small eccentricities). The gravity is softened to mimic a hot stellar disk, and varies as the velocity dispersion. The modes are stable when all rings are prograde, but a fraction of only 5% of counter-rotating rings is sufficient to make unstable modes appear. Sambhus & Sridhar (2002) built a model of the M31 nucleus with counter-rotating orbits in a razor thin nucleus, and checked that this amount of counter-rotation could be compatible with observations. The counter-rotating stars could come from a past accreted system, like a globular cluster.

Bacon et al (2001) explored by N-body simulations the possibility of stable  $m = 1$  mode to explain the M31 eccentric nuclear disk. They found that for a disk mass accounting for  $\sim 20 - 40\%$  of the total central mass, self-gravity is sufficient to counteract the differential precession of the disk. An external perturbation can excite this mode, and it is then long-lasting, over 100 Myr, or 3000 rotation periods. The prograde mode found in the simulations compares well with the  $p$ -modes of Tremaine (2001). There is a remarkable agreement between the observed ( $\sim 3\text{ km s}^{-1}\text{ pc}^{-1}$ ) and predicted value of the pattern speed, in spite of all approximations, and although the WKB approximation is not satisfied.

Although the slow modes are long-lived, their exciting mechanisms should be found, to explain the high frequency of the phenomenon. The dynamical friction of the  $m = 1$  wave on the stellar bulge has been proposed by Tremaine (1995) as an amplification mechanism, if its pattern speed is sufficiently positive. This amplification results from the fact that the friction decreases the energy less than the angular momentum. The orbits with less and less angular momentum are more and more eccentric, and the  $m = 1$  mode develops. Although the efficiency of the mechanism has not been proven, it should not apply for the slow modes considered here, in a slightly rotating bulge. An external perturbation is more likely to trigger the  $m = 1$  perturbation. There is the possibility of infalling of globular clusters, through dynamical friction, a mechanism explored in the next section. Also interstellar gas clouds should be continuously infalling onto the center, since within 10-100 pc of M31 nucleus, dust lanes, and CO molecular clouds are observed (Melchior et al. 2000). The interval between two such external perturbations (either passage of a globular cluster, or a molecular cloud) in M31 is of the same order of magnitude, so that the external perturbations are an attractive mechanism.

Each episode of  $m = 1$  waves will heat the disk somewhat, but the instability is not very sensitive to the initial radial velocity dispersion. Over several  $10^8$  yr periods, the nuclear disk could be replenished by fresh gas from the large-scale M31 disk and subsequent star formation. The hypothesis of cold gas accretion from the disk of M31 itself, has then not only the advantage to trigger the  $m = 1$  perturbation, but also to explain the maintenance of a rather thin and cold nuclear disk.

#### 4.2 *Double nuclei by infalling bodies*

One solution to the double nuclei problem is to assume that dense stellar systems, like globular clusters, or a dwarf satellite, or even black holes, are regularly infalling into the galaxy center, and are responsible for the observed

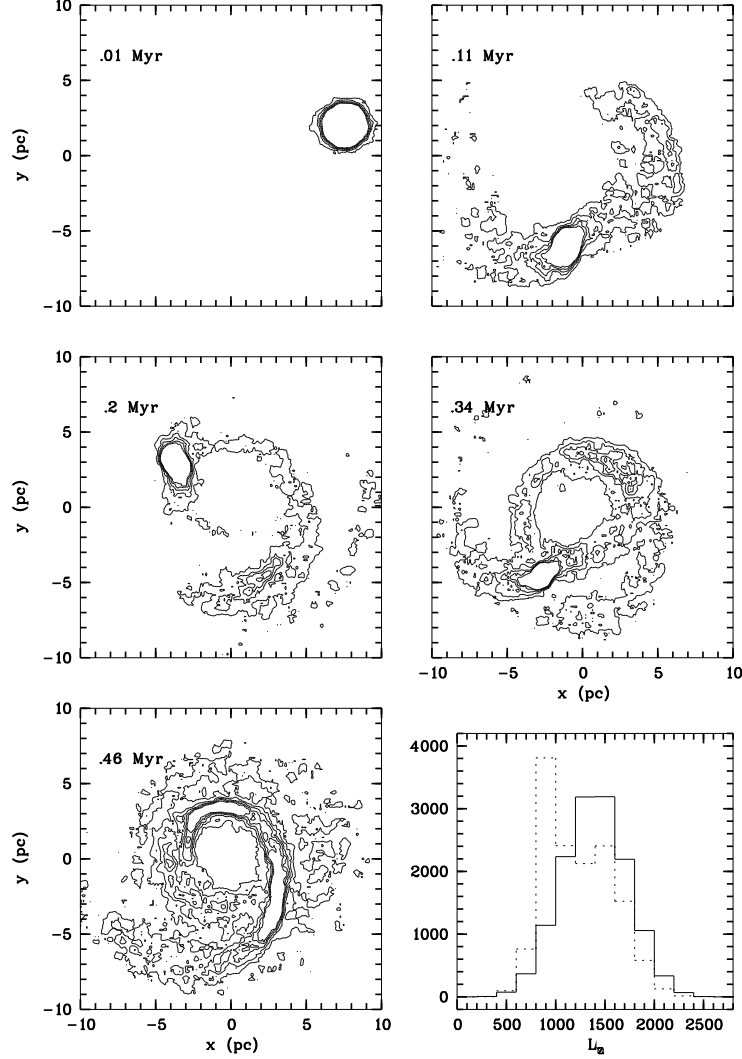


Fig. 21. Simulation of a globular cluster infall towards a galaxy nucleus containing a massive black hole, fit to the M31 characteristics. The panels show the face-on view contours from the cluster stars, from the start to 0.46 Myr. The bottom right panel shows the histogram of the angular momentum for the cluster particles at the beginning (solid line) and at the end (dashed line) of the simulation. From Emsellem & Combes (1997).

morphology. Although the events may be relatively rare, their actual frequency is not well-known, and the question remains open as to a possible fit to the observations.

The typical dynamical friction time-scale, for an object of mass  $M$  at about 10pc from the center, in a spiral galaxy with a bulge of  $\sim 10^{10} M_{\odot}$ , typical of an Sb galaxy like M31, is  $\sim 10^7 (10^6 M_{\odot} / M)$  yr, and it could be much smaller inside. Although short with respect to galactic time-scales, this is much larger than the orbital time of  $3 \times 10^5$  yr at this radius. Tremaine et al (1975) precisely proposed that the central stellar nuclei in spiral galaxies are

the results of many globular clusters infalling by dynamical friction. Typically nuclear stellar systems of  $10^7$ - $10^8$   $M_\odot$  would require the infall of a hundred globular clusters. In this frame, the frequency of the event is relatively large, and could be compatible with the observations.

N-body simulations of globular clusters or dwarf galaxies infalling through the gravitational field of a disk, a bulge, and/or a central black hole, have been carried out by many authors (e.g. Charlton & Laguna 1995, Johnston et al 1999, Combes et al 1999, Bekki 2000b), and applied to explain the M31 nucleus morphology (Emsellem & Combes 1997, Quillen & Hubbard 2003). N-body simulations demonstrate that the infalling system is destroyed by the tidal forces of the black hole at the right distance of the nucleus (about 3pc). The debris then rotate around the nucleus in eccentric orbits, and form an eccentric disk. Several hypotheses can then be explored: either the infalling system is alone able to form the nuclear disk (Bekki 2000a), but then its mass corresponds more to the core of a dwarf galaxy having merged recently with the big primary (a quite rare event). Or the infall of the system excites an eccentric mode in the nuclear disk (Bacon et al 2001), as proposed by Tremaine (1995). Also, the presence of the infalling system not yet diluted in the nuclear disk increase the asymmetry. The details of the dynamics, and in particular the inclination of the nuclear disk with respect to the main disk of M31, or the shift of the velocity dispersion peak from the black hole position, due to the systematic rotation of the luminosity peak of the disk, are all explained by the model by Emsellem & Combes (1997), see Fig. 21.

The nature of the infalling system is constrained by the present metallicity and colors of the nuclear disk, especially if the assumption is made that the infalling system is the first one and forms totally the nuclear disk (Bekki 2000a). The observed colors of the double luminosity peaks in M31 are quite similar to the nuclear disk ones, and different from the bulge, so the hypothesis that the nuclear disk is formed from the infalling systems themselves is possible. The hypothesis of globular clusters is more likely, in the sense that the probability to observe it is larger, the friction time-scale being longer, and it requires at least 25 globular clusters to form the nuclear disk. The hypothesis of a dwarf galaxy merger does not correspond to the quite un-perturbed state of the M31 disk. There is some evidence of a past merger around M31, in the shape of an extended stellar disk, loops and shells (Ibata et al 2001, Irwin et al 2005). However, the time to form these stellar streams is much longer than the time-scale for the galaxy core to infall to the center.

It is interesting to discuss in this context the case of the double nucleus in NGC 4486B, which is thought to be similar to the M31 case, but with larger masses, and larger separation (Lauer et al 1996). NGC 4486B is a compact elliptical galaxy, in the outer envelope of M87 in the Virgo cluster. The double nuclei are separated by 12pc, and produce two almost equal luminosity peaks

at similar distance from the photo-center, so creating almost no lopsidedness in projection. If explained by a nuclear disk, it is of very small eccentricity. The hypothesis of a past merger as the origin of the two stellar nuclei is weaker in this case, since the environment of the cluster center does not favor mergers.

The idea of infalling systems can be generalized to all galaxy mergers as the origin of lopsidedness. In particular, mergers of galaxies could naturally form eccentric disks. The disk would come from the disruption by tidal forces of one of the stellar core. The presence of massive black holes in each spiral galaxy with bulge, strongly supports this scenario. The end steps of the merger process would form a binary black hole. The destruction of nuclear stellar systems by the tidal forces of the black holes led Merritt & Cruz (2001) to suggest that the existence of low-density cores (and not cusps) in giant galaxies is the consequence of mergers. Further simulations of mergers with central black holes should be performed to explore the formation of eccentric disks.

Somewhat larger-scale asymmetry on scales  $\sim 1$  kpc is also seen in mergers of galaxies and is deduced to be long-lived, as discussed in Section 5.3.

### 4.3 Core wandering

Some of the nuclear lopsidedness might also be explained through a special oscillation of the central black hole, called "core wandering". This name came from the physics of globular cluster, that was observed to reveal slow oscillation, with a time-scale larger than the crossing time in numerical simulations (Makino & Sugimoto 1987). Miller & Smith (1992) showed by a large series of numerical simulations that a massive nucleus cannot coincide with the mass centroid of its galaxy in a stable way. The type of instability, where the motion of the nucleus implies potential distortions in the center, which trap more particles, is overstable, and reaches a saturation limit. The phenomenon is local, and the time-scale of the oscillation of the nucleus is of the same order as the central dynamical period (cf Figure 22). This core wandering appears physical, and not the consequence of a  $N^{-1/2}$  random noise oscillation, as tested by simulations with highly varying particle number. In that case, the perturbation amplitude that starts the growth is indeed depending on  $N$ , but not the limiting amplitude, nor the growth rate, which is always a few dynamical times. The  $N^{-1/2}$  phenomenon can be hard to distinguish in small- $N$  simulations, and in globular clusters (Sweatman 1993), but this is not the case for galaxies.

The stochastic part of the core wandering phenomenon has been modeled by Chatterjee et al (2002), separating the force on the central mass in the collective action of the stellar system in which it is embedded, and the fluctuating

stochastic force provided by individual stellar encounters. This second force produces a Brownian motion of the central point mass. These motions occur on a time scale much shorter than the time-scale of evolution of the stellar system.

As for the coherent modes of the stellar system coupled to the central mass, the growing oscillation looks like a density wave, and the saturation amplitude of the motion reaches a galaxy core radius. This unstable phenomenon involves the nucleus, even if there is no central black hole in the center, and is also observed in dynamical friction experiments, when the decay of a satellite is studied (e.g. Bontekoe & van Albada 1987). The limiting amplitude of the nucleus oscillation is then reached from above. This kind of oscillation is also observed in spherical galaxies, and continues to develop for a Hubble time (Miller & Smith 1994).

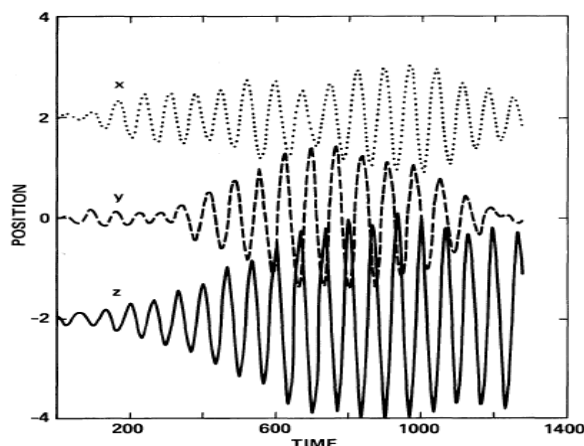


Fig. 22. Evolution with time of the three coordinates of the “nucleus” consisting in the central 1024 particles, selected from an N-body simulation of 100 352 particles. The saturation of the amplitude of oscillations is visible. From Miller & Smith (1992).

Taga & Iye (1998a) studied the oscillations of a central massive black hole in a rotating galaxy, and also confirmed that the phenomenon is not an  $N^{-1/2}$  random noise effect, but a true physical phenomenon. They found by N-body simulations that a massive central body can undertake long-lasting oscillations, but only when its mass is lower than 10% of the disk mass. This produces disk oscillations around it. Crucial must be the rotation of the pattern around the center, since it does not vary its amplitude, when the number of particles change. The disk oscillations occur only when the black hole is allowed to move, when the black hole is artificially nailed down to the center, the disk oscillations vanish. They also conclude that the mechanism at the origin of this instability is a density wave, with a fixed pattern as a function of radius.



When the disk around the central mass is fluid, an instability akin to the one proposed by Shu et al (1990) is possible, with a feedback provided by reflection on a sharp edge in the outer disk. Heemskerk et al (1992) estimate that the edge effect is artificial, and studied instead an  $m = 1$  instability arriving only when the masses of the central object and the disk are comparable. There can be angular momentum exchange between the mass and the disk. To simplify their model, they considered only a gaseous disk with a central gap. This instability is confirmed by Woodward et al (1994), and requires the coupling with the central mass, which is displaced from the center, and moves along a smooth, tightly wound, spiral trajectory. Tago & Iye (1998b) found that the sharp edge condition is not necessary, and that an eccentric instability develops in a stellar disk, provided that the central mass is smaller than the disk mass (about 10%), and it is mobile. The eccentric instability then develops a one-arm spiral, with an amplitude that is stronger than when the central mass is fixed to the center. The mechanism is strongly dependent on the softening used, and should be local to the central parts.

#### 4.4 *Other mechanisms*

If a normal disk around a black hole is not spontaneously unstable to  $m = 1$  perturbations, the modifications of the stellar distribution function  $F$ , and in particular the depletion in low-angular momentum orbits, leading to the empty loss-cone phenomenon, can provide the source of instability. If the derivative of  $F$  with respect to  $J$  is positive, then spherical near-Keplerian systems are neutrally stable (allowing the displacement of the nucleus with respect to central mass), and the flattened non-rotating systems are unstable to  $m = 1$  modes (Tremaine 2005).

Peiris & Tremaine (2003) construct eccentric disk models to represent the double nucleus in M31, and claim that the inner nuclear disk must be inclined by at least 20 degrees with respect to the main disk of the galaxy to represent the data. Although their model is only dynamical, and does not include all the physics, with self-gravity, etc. , this suggests that the lopsidedness might be related to a warp or a misalignment. The latter could be the source of dynamical friction against the bulge, and relatively rapid alignment should ensue. A possibility is that the bulge is itself misaligned with the main galaxy disk, which could be due to a recent galaxy interaction (e.g. Ibata et al 2001, Block et al 2006).

Salow & Statler (2001, 2004) compute a more sophisticated model, including self-gravity. They populate quasi-periodic orbits for stars, in the rotating frame with a constant precession speed. The eccentricity of the orbits change sign with radius, so that the apocenter of the orbits change phase in the plane

of the nuclear disk (cf fig 23). The resulting best fit model is similar to that obtained with N-body simulations of a strong  $m = 1$  mode in a cold thin disk with a central black hole (Bacon et al 2001). In particular the pericenters of the orbits in the inner and outer disks are in phase opposition. The precession rate, however, is rapid ( $\Omega = 36.5 \text{ km s}^{-1} \text{ pc}^{-1}$ ).

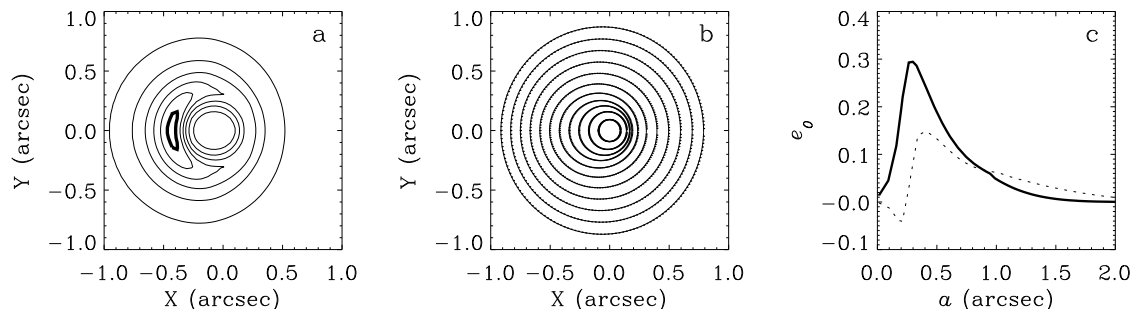


Fig. 23. (a) Density contours of the best-fit model of the M31 eccentric disk, the central black hole being at  $(X,Y) = (0,0)$ ; (b) uniformly precessing orbits in the total potential. (c) the radial variation of the eccentricity  $e$  of orbits, as a function of semi-major axis  $a$ : *dotted line*– the orbit model, with eccentricities changing sign with radius; *full line* – as a consequence of disk self-gravity, the eccentricity does not change sign any longer. From Salow & Statler (2004).

## 5 Lopsidedness in galaxies in groups, clusters and mergers

### 5.1 Lopsidedness in galaxies in groups

Tidal encounters between galaxies in groups are more probable given the higher number density and the consequent frequent interaction between galaxies in groups. Further, these have relative velocities similar to the field galaxies, hence the lopsidedness arising due to a response triggered by tidal encounters is more likely to occur in these. This is in fact borne out by the observations of Hickson group galaxies (Rubin et al. 1991) where a large fraction ( $> 50\%$ ) of galaxies show lopsided rotation curves. This is much higher than the case of field spiral galaxies where only  $\sim 25\%$  show asymmetric rotation curves (Rubin et al. 1999, Sofue & Rubin 2001). The observation of rotation curves of 30 galaxies in 20 Hickson groups (Nishiura et al. 2000) confirms this higher frequency. In another study involving HI observations, all the five major spirals in the nearby Sculptor group of galaxies (Schoenmakers 1999) show kinematical lopsidedness, and two show morphological elongation or asymmetry. A multi-wavelength study of two group galaxies NGC 1961 and NGC 2276

shows evidence for lopsidedness which has been attributed to tidal interactions (Davis et al. 1997).

The two-dimensional maps of HI have been Fourier-analyzed recently to obtain the  $m=1$  Fourier amplitudes and phases for a sample of 18 galaxies in the Eridanus group (Angiras et al. 2006). This is the first quantitative analysis of asymmetry in the surface density distribution of the HI gas, and is similar to the Fourier analysis now done routinely in the literature for the near-IR data representing old stars in galaxies.

The group location of this sample allows us to serendipitously study the lopsidedness in a group setting. The galaxies studied show a higher magnitude of asymmetry than the field galaxies, and also a higher fraction of galaxies show asymmetry. The average amplitude of lopsidedness measured for the Eridanus group galaxies is nearly twice that in the field galaxies over the same radial range of 1.5-2.5 disk scalelengths. Second, nearly 30 % of the sample galaxies show lopsidedness amplitudes three times larger than the field average of 0.1. Fig. 24 shows the results for two galaxies UGC 068 and NGC 1325, in the Eridanus group.

The asymmetry is measured in this case to over twice the radial distance that is typically covered in the near-IR studies (e.g. Bournaud et al. 2005 b). This is because the tracer used here is HI which extends farther out than the stars, and because the sky background limits the Fourier analysis in the near-IR to  $\sim 2.5$  disk scalelengths.

The  $A_1$  values measured from the HI data and the R-band data are available for four galaxies, and these were compared. It was found that in the radial region of overlap, the two tracers show a similar value of lopsidedness, see Fig. 25. This confirms that the origin of lopsidedness in HI is of a dynamical origin and not purely of a gas-dynamical process that only applies to the gas.

A similar Fourier analysis has been done for a sample of 12 galaxies in the Ursa Major (Angiras et al. 2007) by analyzing the 2-D HI data (Verheijen 1997) available for these. The average value of lopsided amplitude in the 1.5-2.5 disk scalelength region in this sample is smaller than in the Eridanus group, and is closer to the field galaxies case, as shown in Fig. 26. This could reflect the different spatial distribution of galaxies in the two groups- the ones in the Ursa Major are distributed along a filament.

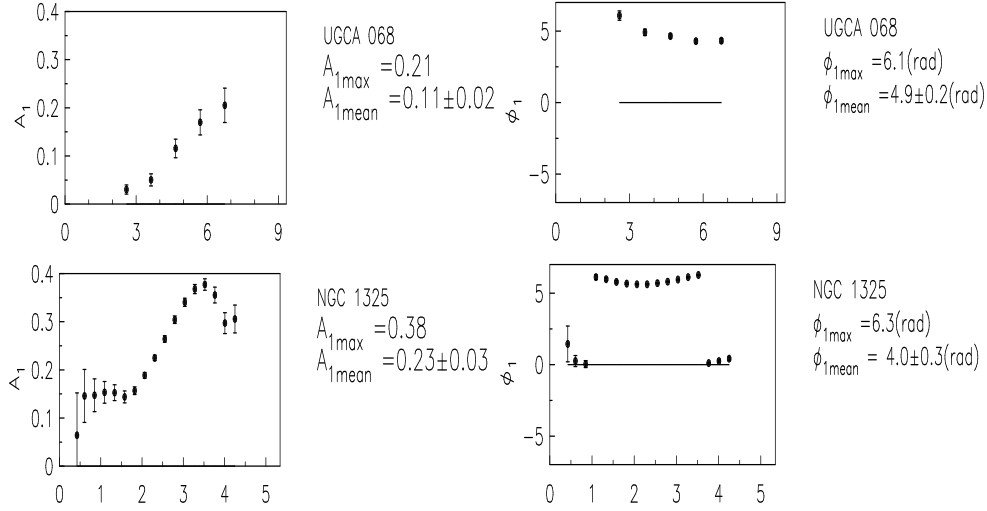


Fig. 24. The lopsided amplitude and phase of the HI surface density distribution versus radius for the two galaxies UGC068 and NGC 1325 in the Eridanus group, taken from Angiras et al. (2006). The amplitude increases with radius and the phase is nearly constant indicating that  $m=1$  is a global mode. The lopsidedness in the HI can be measured until several disk scalelengths, more than twice the radial distance possible for the stars.

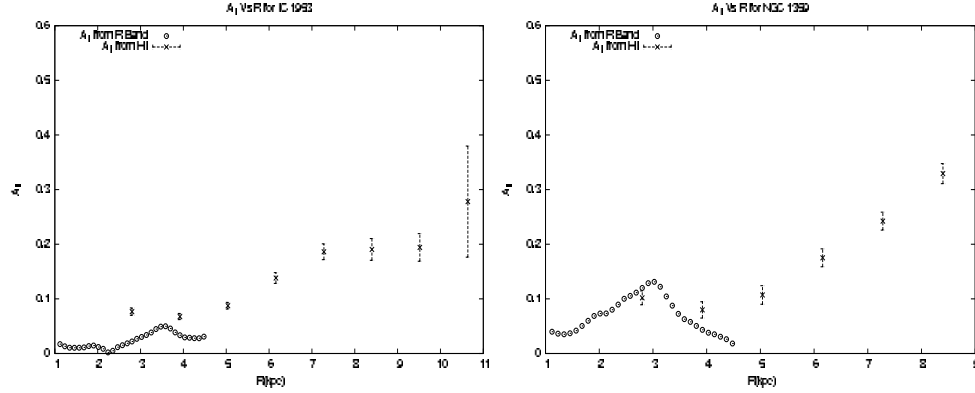


Fig. 25. A comparison of the lopsided amplitude  $A_1$  obtained by analyzing the HI data and the R-band data for stars for NGC 1953 (left panel) and NGC 1359 (right panel), from Angiras et al. (2006). In the radial region of overlap the values are comparable, thus indicating the same origin for the lopsidedness both in stars and gas. The figures also strikingly illustrate that HI is a much better tracer than stars for the study of lopsidedness at large radii.

An interesting characteristic of lopsidedness in group galaxies as noted by Angiras et al. (2006) is that the early-type galaxies show a higher quantitative lopsidedness than do the late-type galaxies, see Fig. 27. This is opposite to what is seen in the field galaxies (Bournaud et al. 2005b) and indicates that

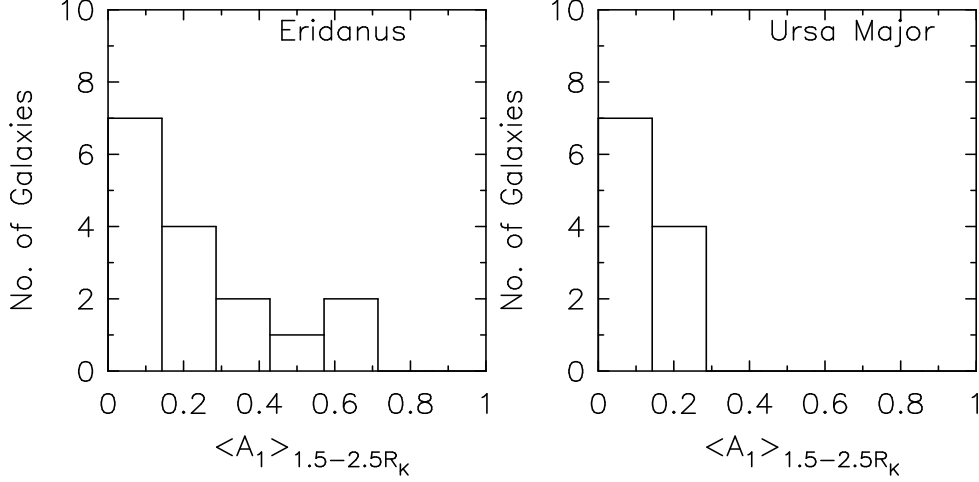


Fig. 26. The histograms denoting the number of galaxies vs. the lopsided amplitude measured in the 1.5-2.5 disk scalelength range for the Ursa Major Group (left) and the Eridanus group (right) of galaxies, taken from Angiras et al. (2007). The galaxies are more lopsided in the Eridanus group, indicating a substantial variation between groups.

tidal interactions play a dominant role in generating lopsidedness in the group galaxies. This is not surprising given the high concentration of galaxies in a group. Tidal interactions would tend to cause a secular evolution of galaxies to an earlier type and hence when these are the dominant mechanism for generating lopsidedness, one would expect higher values of lopsidedness for early-type galaxies, as argued by Bournaud et al. (2005 b).

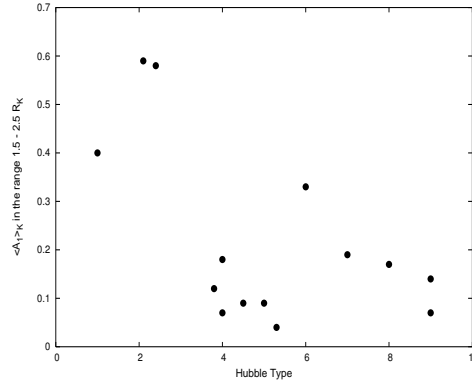


Fig. 27. The lopsided amplitude measured between the radial range of 1.5-2.5 disk scalelengths vs. the galaxy type, from Angiras et al. (2006). The early-type galaxies show a higher lopsidedness than the late-type galaxies. This is opposite of what is seen for the field galaxies, see Fig. 5.

A distinguishing feature of asymmetry in the group galaxies is that the values of the asymmetry as measured by the mean fractional Fourier amplitudes  $A_1$ ,  $A_2$  and  $A_3$  for the modes  $m=1,2$  and 3 are found to be comparable (Angiras et

al. 2007). Also, the derived perturbation potential parameters  $\epsilon_1$ ,  $\epsilon_2$  and  $\epsilon_3$  are found to be comparable. Although this last result depends on the model used, it reinforces the similar result obtained for the Fourier amplitudes which are directly observed and hence are model-independent (Section 3.1.2). This is in contrast to the field galaxies where  $A_1$  and  $A_2$  are comparable and are generally stronger than  $A_3$  and the other higher mode amplitudes (Rix & Zaritsky 1995). This indicates the importance of multiple, simultaneous tidal interactions that can occur under the special conditions of a group environment. This needs to be studied by future dynamical studies including by N-body simulations. Since tidal interactions are frequent, occurring on a timescale of  $< \sim 0.5 Mpc/300 \text{ km s}^{-1} \sim 3 Gyr$ , the long-term maintenance of lopsidedness is not a problem in this environment.

## 5.2 *Lopsidedness in galaxies in clusters*

The galaxies in clusters may undergo even more frequent encounters than in the groups because of the generally higher number density of galaxies. However the relative velocity between galaxies is higher in clusters and hence the encounters are weaker in strength. The accumulation of a large number of weak interactions has been called the galaxy harassment (Lake, Katz, & Moore 1998). The asymmetry in NGC 4252 including the smoothly varying HI velocity field along the tidal tail, has been attributed to this effect (Haynes, Giovanelli & Kent 2007). The amplitude of lopsidedness generated due to tidal encounters is expected to be weaker in this case because of the quick encounters. On the other hand, other dynamical processes such as asymmetry arising due to ram pressure may be specifically applicable in a group or a cluster setting. This may even be the dominant source of gas asymmetry in these and can affect the HI gas lying on the outer parts of a galactic disk. An interesting interplay of these various effects is possible as in NGC 4848 in the Coma cluster, which shows a lopsided distribution of the molecular gas (Vollmer et al. 2001). This has been explained by the interaction between the galactic gas, and the gas removed by ram pressure stripping around  $4 \times 10^8$  yr ago which is now falling back.

Since the cluster galaxies often show HI deficiency especially in the outer parts where lopsidedness is generally more common, this could be a potential problem with detecting lopsidedness in cluster galaxies.

Despite this, in some galaxies of groups and clusters, the gas alone is known to show a strong asymmetry - as in NGC 4647 (Young et al. 2006). This strong gas asymmetry has been frequently attributed to ram pressure stripping. However, the role of the gravitational potential asymmetry in lopsidedness cannot be neglected, even in these cases.

### 5.3 *Lopsidedness in centers of advanced mergers*

A fairly new regime that is just beginning to be explored is the asymmetry at the centers of advanced mergers of galaxies. A recent systematic study was done by Jog & Maybhat (2006), with a view to understand the mass asymmetry and the relaxation in the central regions of mergers.

Interactions and mergers of galaxies are known to be common and significantly affect their dynamics and evolution. The outer regions of merger remnants covering a distance of  $\sim$  few kpc to a few 10 kpc have been well-studied. These can be fit by an  $r^{1/4}$  profile (class I), an outer exponential (class II) or a no-fit profile (class III) (Chitre & Jog 2002), and the first two can be explained as arising due to equal-mass mergers (e.g., Barnes 1992) or unequal-mass mergers (Bournaud, Jog & Combes 2005 a) respectively, while the third class corresponds to younger remnants. Despite its obvious importance for the evolution of the central regions, the luminosity distribution in the central regions of mergers was not studied systematically so far. A few mergers where this has been studied, such as NGC 3921 (Schweizer 1996), and Arp 163 (Chitre & Jog 2002), show wandering or meandering centres for the consecutive isophotes.

Jog & Maybhat (2006) chose a sample of 12 advanced mergers which showed signs of recent interaction such as tidal tails or loops but had a merged, common center and covered all three classes discussed above; and the angular size of the galaxy was sufficiently large to allow the Fourier analysis by dividing the image into a few radial bins. The sample was chosen so as to cover the three classes showing different remnant profiles as described above. The  $K_s$  band images from 2MASS were analyzed using the task ELLIPSE in STSDAS. The elliptical isophotes were fitted to galaxy images while allowing the center, ellipticity and the position angle to vary so as to get the best fit. Fig. 28 (top panel) shows the result for Arp 163. The isophotes are not concentric, instead the centers  $(X_0, Y_0)$  of consecutive isophotes show a wandering or sloshing behaviour, indicating an unrelaxed central region.

Another measure of asymmetry is the lopsidedness of the distribution, to obtain this a galaxy image was Fourier-analyzed with respect to a constant center and the amplitude  $A_1$  and the phase  $p_1$  of the  $m = 1$  mode were plotted versus radius- as shown for Arp 163 in the lower panel of Fig. 28. During the Fourier analysis the center was kept fixed, for the reason as discussed in Section 2.1.2. The intensity and hence the mass distribution is highly lopsided with the fractional amplitude for the  $m=1$  mode of  $\sim 0.15$  within the central 5 kpc.

All the sample galaxies show strong sloshing and lopsidedness in the central regions. The asymmetry does not seem to significantly depend on the masses of

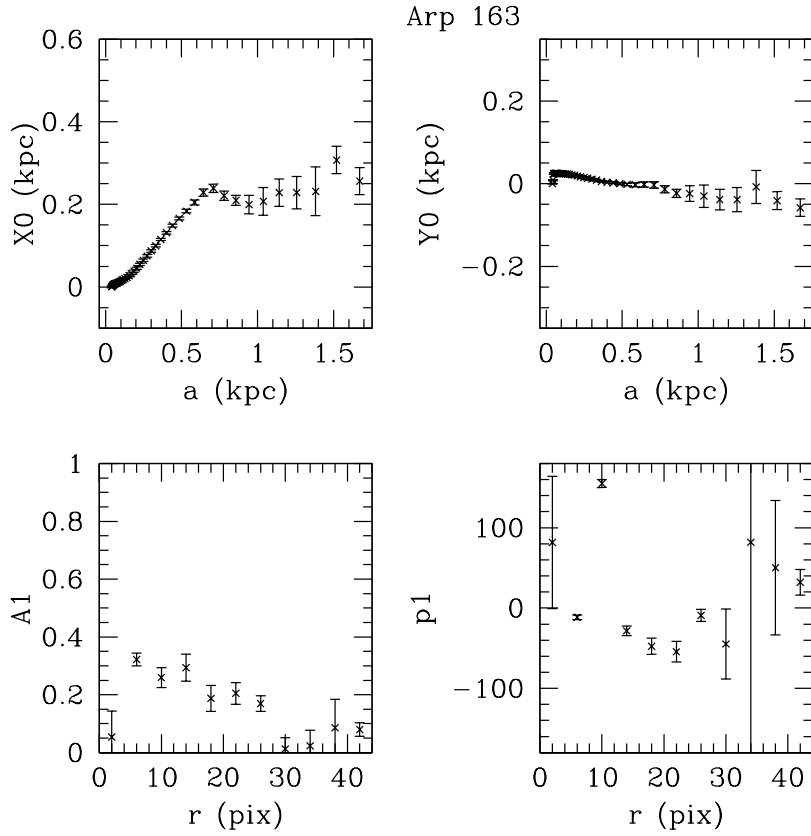


Fig. 28. Central region of the merger Arp 163 - The top panel shows the centers of the isophotes vs. the semi-major axis: the centers show a sloshing pattern indicating an unrelaxed behaviour. The lower panel shows the Fourier amplitude  $A_1$  and the phase  $p_1$  vs. radius for the lopsided mode ( $m = 1$ ): the lopsided amplitude is large and the phase fluctuates with radius. This is taken from Jog & Maybhate (2006).

progenitor galaxies - being similar for class I and II cases. However, it is higher for the mergers in early stages of relaxation (class III). The corresponding values especially for the central lopsidedness are found to be smaller by a factor of few for a control sample of non-merger galaxies. This confirms that the high central asymmetry in mergers is truly due to the merger history.

The ages of remnants are deduced to be  $\sim 1$ -2 Gyr as seen from the remnants with similar outer disturbed features in the N-body simulations of mergers



(Bournaud et al. 2004), during which time these are likely to get chosen as our sample galaxies.

Thus the central asymmetry is long-lived, lasting for  $\sim 100$  local dynamical timescales. Hence it can play an important role in the dynamical evolution of the central regions. First, it can help fuel the central AGN since it provides a means of outward transport of angular momentum. Second, it can lead to the secular growth of the bulges via the lopsided modes. These need to be studied in detail theoretically. Since this predicted evolution is due to the central asymmetry that is merger-driven, this process could be important in the hierarchical evolution of galaxies.

## 6 Related topics

### 6.1 Relative strengths of lopsidedness ( $m=1$ ) and bars/spiral arms ( $m=2$ )

Nearly all physical mechanisms, such as a tidal encounter or gas accretion, that can give rise to an  $m=1$  mode will also give rise to an  $m=2$  mode. Which of these two dominates depends on the detailed parameters of the system. For example, for a distant encounter, the  $m=2$  mode is stronger. A prograde encounter is likely to preferentially generate the  $m=2$  mode while a retrograde encounter favours the generation of a lopsided ( $m=1$ ) mode (Bournaud et al. 2005 b).

It is well-known that a two-armed spiral pattern is supported as a kinematical feature over most of the galactic disk, or in the region of nearly flat rotation curve in general, since the pattern speed given by  $\Omega - \kappa/2$  is nearly constant in this case (Lindblad 1959). The density wave theory of spiral features is built around this idea (Rohlfs 1977).

The human eye/ brain likes to notice bisymmetry. This is one reason why the two-armed spirals have received enormous amount of attention in the theory of galactic structure and dynamics. This is despite the fact that it has been known for a long time that a higher  $m$  value or a flocculent behaviour is more commonly observed in galaxies (see e.g., Elmegreen & Elmegreen 1982).

It should be noted that the early observational studies of spiral structure such as the Hubble atlas (Sandage 1961) used blue filter where the emission from the young stars stands out, and also the dust extinction plays a major role in the galaxy image produced. In contrast, the more recent studies using the near-IR band data, in particular in the  $K_s$  band avoid this problem and trace more accurately the underlying old stellar mass population (e.g., Block et al.

1994, Rix & Zaritsky 1995). Interestingly, in their recent study leading to the Large Galaxy Catalog, Jarrett et al. (2003) show that  $m=1$  is the most common mode seen in the near-IR. They argue that, as noted by Block et al. (1994), there is theoretical reason to believe that  $m=1$  modes should dominate the internal structure of spirals.

The question then is, why is there a prevalent notion even amongst professional astronomers that lopsidedness is unusual in a galaxy while a two-armed spiral is the norm, which is totally in contrast to the observed case. We think one reason for this wrong notion could be that the phase of lopsidedness is observed to be nearly constant (see Section 2.3). Thus the resulting isophotal contours are oval-shaped or egg-shaped, and their elongation is not striking in the inner or optical parts of a galaxy, so an untrained eye may miss it.<sup>2</sup> If there were a strong radial dependence of the phase, then the resulting one-armed structure as it occurs in M51 or NGC 4564 would be easy to see.

The amplitude of lopsidedness is found to increase with radius for the stars (Rix & Zaritsky 1995) and for HI gas (Angiras et al. 2006, 2007). This is the reason why even a low-sensitivity HI map reveals the lopsidedness easily - see e.g. the images of a face-on galaxy like M101 or an edge-on galaxy like NGC 891 (Baldwin et al. 1980). Thus it is not surprising that lopsidedness was first detected in the HI maps. The fact that it is now found to be equally ubiquitous in the older stars as well, is what makes its study even more important and challenging. For example, it points to a basic dynamical mechanism for the origin of lopsidedness, and not something based purely on the gas dynamical processes. An interesting feature regarding observational detection of lopsidedness, first noted by Rix & Zaritsky (1995), is that it does not get confused with the inclination angle, unlike the  $A_2$  values.

### 6.1.1 *Observed amplitudes of $m=1$ and $m=2$ components*

The observed amplitudes  $A_1$  and  $A_2$  of  $m=1$  and 2 respectively for stars are generally comparable, and both are much larger than the values for the higher  $m$  modes for the field galaxies (Rix & Zaritsky 1995, Bournaud et al. 2005 b). Normally  $m=2$  is taken to denote a bar or a spiral arm in the inner or outer regions respectively, or it can also denote disk ellipticity. The amplitudes for  $m=2$  have been measured for larger samples (Laurikainen, Salo, & Rautiainen 2002, Buta et al. 2005, Bournaud et al. 2005 b). The average values of  $A_1$  and  $A_2$  between 1.5 - 2.5 disk scalelengths have been measured for the 149 galaxies in the OSU catalog (see the Appendix in Bournaud et al. 2005 b), and the two generally show a positive correlation (see Fig. 8 in that paper). This cannot be explained if the tidal encounters were the main generating

---

<sup>2</sup> On the other hand, a little training or awareness allows one to detect lopsidedness in galaxies easily, as the authors of this present article have found !

mechanism since  $m=2$  spiral arms or bars are more easily triggered on direct orbits where  $\Omega - \kappa/2$  is positive (e.g., Gerin et al. 1990). In contrast, a lopsided mode is more likely to be triggered or last longer in a retrograde orbit since the pattern speed of  $m=1$  asymmetries,  $\Omega - \kappa$ , is negative in a galactic disk. The simulations by Thomasson et al. (1989) shows that retrograde tidal encounters between galaxies lead to the formation of leading one-armed spiral arms, as in NGC 4622. Observationally very few galaxies show a leading arm. Pasha (1985) found that only 2 out of the 189 galaxies studied show a leading arm (NGC 3786, NGC 5426), and each of these happen to be in a pair, which agrees with the work by Thomasson et al. (1989). It is possible that the pattern speed of  $m=1$  arms in other galaxies is small - this has to be checked observationally. As discussed in Section 3.2.3 this can have a bearing on the mechanism for the origin of lopsidedness. For example, if the pattern speed is small, the global modes are long-lived (Saha et al. 2007) and do not need to be triggered frequently.

On the other hand, the galaxies in groups show a higher lopsidedness for the early-type galaxies, and show a comparable magnitude for all the lower modes,  $m=1,2$ , and 3. The frequent and even concurrent tidal encounters in this setting are probably responsible for this (see Section 5.2).

The different modes could interact directly but this obvious line of research has not been followed up much. A non-linear coupling between  $m=1,3$  and  $m=2$  was proposed by Masset & Tagger (1997) for the central regions. Even though the  $m=1$  mode is largely seen in the outer galactic disk while the bars and the spiral structure ( $m=2$ ) are seen more in the inner parts of a galactic disk, they can still have a dynamical effect on each other. The heating due to a bar ( $m=2$ ) can suppress the further growth of a lopsided mode, as was seen in the numerical simulations for a purely exponential disk by Saha et al. (2007). Conversely, the presence of a lopsided mode can lead to a bar dissolution as has been studied by Debattista & Sambhus (2008). This topic needs more study and could shed an important light on the dynamical evolution of a disk due to various non-axisymmetric features.

## 6.2 *Asymmetry in the dark matter halo*

The study of disk asymmetry including lopsidedness has triggered many applications where the asymmetry is used as a tool to gain information about the shape and the density distribution in the dark matter halo.

The dark matter halo is generally assumed to have a spherical shape, for the sake of simplicity. This view has been challenged, and there have been studies which have used various tracers such as the polar rings (Sackett & Sparke

1990), warps (e.g. Ideta et al. 2000), gas flaring (Olling 1996, Becquaert & Combes 1997, Narayan, Saha & Jog 2005, Banerjee & Jog 2008), to deduce the shape of the dark matter halo in galaxies. A summary of topic is given in Natarajan (2002).

In the tidal picture of the origin of disk lopsidedness, the disk responds to a distorted dark matter halo. Thus we can use the observed disk asymmetry to deduce the asymmetry in the galactic plane of the dark matter halo, which is not visible directly. As discussed in detail in Section 3.2.1, the observed disk lopsidedness can be used to deduce the halo lopsidedness and indicates a few % lopsidedness for the halo in a typical galaxy. Similarly, on treating a self-consistent disk response, and using the disk ellipticity, one can deduce the ellipticity of the dark matter halo (Jog 2000). The idea of negative disk response (Jog 1999, 2000) has been applied by Bailin et al. (2007) for a more realistic radial variation of the ellipticity of the potential to show that the disk response circularizes the net potential in the central region of a triaxial halo.

The amplitude of lopsidedness is higher in the group galaxies and can therefore imply a higher distortion of the halo,  $\sim 10$  % as shown for the case of the Eridanus group galaxies (Angiras et al. 2006). The power in the various  $m$  modes is comparable (see Schoenmakers 2000, Angiras et al. 2007). The values of all three perturbation potentials derived  $\epsilon_1, \epsilon_2, \epsilon_3$  are comparable (Section 5.1). This can be an important clue to the mechanism for generating lopsidedness in groups, and perhaps indicates the importance of multiple, simultaneous tidal interactions that can occur under the special conditions of a group environment.

The asymmetry in the dark matter halo of the Galaxy has been studied quantitatively as follows. The recent survey of atomic hydrogen gas in the outer Galaxy (Levine et al. 2006) has revealed a striking asymmetry in the thickness map of HI gas. The gas in the Northern part flares more with the thickness higher by a factor of  $\sim 2$  compared to that in the South, at a galactocentric radial distance of 30 kpc. This has been modeled by Saha et al (2008), who obtain the vertical scaleheight for the galactic disk in the gravitational field of the dark matter halo by solving the vertical force equation and the Poisson equation together. This model shows that the above asymmetry is best explained by a lopsided dark matter halo, with a small elliptical distortion that is out of phase with the lopsidedness.

The centres of dark matter halos are predicted to show lopsidedness as based on the N-body simulations in the  $\Lambda$ CDM cosmology (Gao & White 2006) and the size of asymmetry is larger for larger size halos as in clusters of galaxies, though these models need to be followed by direct predictions which can be checked against observations as stressed by these authors.

The Fourier harmonic technique developed mainly to study the disk asymmetry (Jog 1997, Schoenmakers et al. 1997) has now been applied to the kinematical data along the minor axis for the dwarf galaxy DDO 47 (Gentile et al. 2005). This study has shown that the velocity dispersion components are too small to arise due to a cusp. Hence the galaxy was deduced to have a genuine core-like density distribution of the dark matter halo in the central regions.

The asymmetry in the halo is expected to be long-lived because of its collisionless nature. However, a finite pattern speed can reduce this life-time to be  $\sim$  a few Gyr, or much less than the Hubble time (see the discussion in Section 3.2.3).

### 6.3 *Comparison with warps*

Spiral galaxies also show a bending of the midplane at large radii, this is known as the warp. A warp is also a global feature of type  $m=1$  except in the vertical direction (Binney & Tremaine 1987). Warps are extremely common and in fact all the main galaxies in the Local group, namely the Galaxy, M31, M33, LMC are warped. Warps are seen mainly in the HI gas, typically beyond a 4-5 disk scalelength radius (Briggs 1990) but in many cases are also seen in stars in a radial region somewhat inside of this (Reshetnikov & Combes 1998).

A tidal encounter in an arbitrary orientation can generate both lopsidedness as well as warps, as is known, see e.g. Weinberg (1995), and Bournaud et al. (2004). Individual galaxies often exhibit both these phenomena, and galaxies with an intermediate angle of inclination allows both to be seen easily as in NGC 2841 (see Fig. 1b in the present paper). Both the features share some common properties - namely they are seen preferentially in the outer parts of a galactic disk, and their long-term maintenance against differential rotation is a problem. The disk self-gravity resists imposed perturbation in the inner parts, as denoted by the negative disk response (Section 3.2.1.c). The resulting net self-consistent disk response shows that the disk will exhibit lopsidedness only outside of  $\sim 2$  disk scalelengths (Jog 1999, Jog 2000). A similar calculation for the perturbation along the vertical direction shows that the onset of warps in a galactic disk occurs only beyond 4-5 disk scalelengths (Saha & Jog 2006).

We note, however, that warps and lopsided distribution are physically different features. First, in a lopsided distribution the centre of mass is shifted with respect to the original centre of mass of the galaxy. On the other hand, in a standard  $m=1$  S-shaped warp, the mass distribution is symmetric with respect to the centre of mass and to the symmetry plane of  $z = 0$ . Second, the onset of warps is determined by a somewhat arbitrary threshold of a few degree lifting

of the mid-plane away from its central value, which is set by the observational detection limits. On the other hand, a lopsided amplitude is well-determined quantitatively following the Fourier analysis- although the threshold value of what constitutes a lopsided galaxy is still fairly arbitrary (see Section 2.2).

#### 6.4 *Implications for high redshift galaxies*

Lopsidedness is more likely at high redshift, since galaxy interactions are more frequent. There is multiple observational evidence of more asymmetric galaxies at high redshift (e.g. Simard et al 2002). Measuring the lopsidedness is however complex due to the clumpy/non-uniform background distribution in a galaxy (e.g. Elmegreen et al 2004), and the overall low spatial resolution.

### 7 **Effect of lopsidedness on galaxy evolution**

A galactic disk is inherently susceptible to the formation of the lopsided mode (Section 3). This mode can be long-lived as evident from the high fraction of galaxies that are observed to show lopsidedness. The dynamical origin and the evolution of these features is a challenging problem as discussed here. But apart from that, does the existence of lopsidedness affect the galaxy in any way? The answer is a resounding yes.

The list of processes whereby a lopsided distribution can affect the evolution of the galactic disk in a significant way include the following:

1. A lopsided distribution can help in the angular momentum transport in the disk and can thus contribute to the secular evolution in the disk. This is especially important given the long-lived nature of the lopsidedness. This can cause a redistribution of matter as studied by Lynden-Bell & Kalnajs (1972). This process is especially important at lower radii because the dynamical timescale is smaller. Hence the net dynamical evolution is likely to occur on timescales less than the age of the galaxy. The details for this process need to be worked out.
2. The fueling of the central active galactic nucleus (AGN) can occur due to the  $m=1$  motion of the central black hole (Section 4.2) and this could be more effective than the first process above.
3. Lopsidedness could affect the details of galaxy formation. For example, the accretion of mass as mediated by  $m=1$  would be especially important for the highly disturbed high redshift galaxies.

4. The lopsided distribution results in an azimuthal asymmetry in star formation in a galactic disk. In a lopsided potential, the effective disk surface density is shown to be a maximum at  $\phi = 0^\circ$ , corresponding to an overdense region, while there is an underdense region in the opposite direction along  $\phi = 180^\circ$ . The fractional increase in surface density at  $\phi = 0^\circ$  is high  $\sim 0.3 - 0.5$  for strongly lopsided galaxies (see Fig. 1, Jog 1997). Thus, the molecular gas in the overdense region could become unstable and result in enhanced star formation, as shown for example for the parameters for M101. Further, the enhanced star formation in the overdense region is argued to give rise to a preferential formation of massive stars (Jog & Solomon 1992). This will result in more HII regions in the overdense region. This prediction is exactly in agreement with observations of more HII regions seen along the SW in M101.

Lopsidedness has also been observed in the  $H_\alpha$  emission from the star-forming regions in dwarf irregular galaxies (Heller et al. 2000). Such asymmetry is expected to be common in all galaxies and we suggest future work in this area is necessary.

## 8 Summary and Future Directions

We have reviewed the spatial and kinematical lopsidedness in a galaxy - both the observations and dynamics, as seen in the various tracers - stars and gas, and in the inner and outer regions, and in different settings- field and group environment.

The lopsidedness is shown to be a common phenomenon. Nearly 30 % of spiral galaxies show a 10% fractional amplitude in  $m=1$  or the first Fourier mode. The amplitude can be higher and can go up to 30 % in strongly lopsided galaxies like M 101. In a group environment, this effect is stronger: all the galaxies show lopsidedness and the average amplitude of lopsidedness is nearly twice that in the field case.

We recommend that the future users adopt the fractional Fourier amplitude  $A_1$  as the standard criterion for lopsidedness. Further, the threshold value that could be adopted could be the average value of 0.1 seen in the field galaxies in the intermediate radial range of  $1.5-2.5 R_{exp}$  (Bournaud et al. 2005 b), so that galaxies showing a higher value can be taken to be lopsided. A uniform criterion will enable the comparison of amplitudes of lopsidedness in different galaxies, and also allow a comparison of the fraction of galaxies deduced to be lopsided in different studies.

A variety of physical mechanisms have been proposed to explain the origin of the lopsidedness, of which the most promising are the ones involving a tidal

encounter, gas accretion, and gravitational instability. A unique feature of the  $m=1$  perturbation in the galactic disk is that it leads to a shift in the centre of mass in the disk, and this further acts as an indirect force on the original centre of the disk. The self-gravity of the perturbation decreases the precession rate by a factor of  $\sim 10$  compared to free precession. The disk is thus shown to naturally support a slowly-rotating, global, lopsided mode which is long-lived. However, the uniqueness of this solution has been proven. Also it is not clear what would give rise to such slow modes, except gas accretion. A fast pattern speed as would occur for lopsidedness generated in a tidal encounter cannot yet be ruled out.

The high fraction of galaxies showing lopsidedness has still not been explained fully. The N-body simulations for a tidal interaction between galaxies with a live halo and gas (Bournaud et al. 2005 b) show that the lifetime of the lopsided mode thus generated is a few Gyr. The other mechanism involving steady gas accretion would probably generate a one-armed lopsided mode which is not seen commonly. Satellite accretion could generate the right amount of lopsidedness but would also thicken the disks more than is seen. It needs to be checked if a small-mass satellite falling in can generate the right amplitude distribution of lopsidedness without thickening the disk, and of course if there are such satellites available to fall in at a steady rate. A measurement of pattern speed in real galaxies would be extremely useful in constraining the main mechanism for generating lopsidedness. For example, a tidal encounter is expected to give rise to a lopsided mode with a small but finite pattern speed.

In group galaxies, the ongoing continuous tidal interaction can help one get over the maintenance problem easily. This can explain why nearly all galaxies in a group are strongly lopsided, and may perhaps explain why these show equal amplitudes of higher asymmetry modes. This needs to be confirmed by detailed dynamical studies and simulations.

Some of the open problems in this field include: a measurement of pattern speed of lopsided mode in real galaxies, the amplitude and thickening of the disk generated by an accretion of a low-mass satellite, and the study of origin and evolution of lopsidedness in galaxies in groups, and the evolution timescale of a  $m=1$  mode in a collisionless dark matter halo. These deal with the origin and the evolution of lopsidedness in galaxies. The related field of problems involving the study of the dark matter shape has much promise, and some work has been started along this direction with models to explain the observed HI thickness distribution. In the central regions of mergers of galaxies, the dynamics of the sloshing and lopsidedness seen on scales of  $\sim 1$  kpc needs to be investigated. On further small scales, simulations with central black holes should be carried out to explore the formation of eccentric disks as in M31.



An even more interesting set of questions has to do with the effect the lopsidedness has on the further evolution of the galaxy. These include: the angular momentum transport, the fuelling of the central active galactic nucleus, enhanced star formation in the overdense regions, and the early evolution of a galaxy mediated by the  $m=1$  mode for the studies of galaxies at high redshift, and the coupling between the various modes (bars, lopsidedness etc) in a galactic disk and its effect on the further dynamical evolution of a galaxy.

In summary, the study of asymmetry is a rich and a challenging area in galactic structure and dynamics, with lots of open questions - both observational and theoretical.

**Acknowledgments:** We are happy to acknowledge the support of the Indo-French grant IFCPAR/2704-1 .

## References

- Abraham, R.G., van den Bergh, S., Glazebrook, K., Ellis, R.S., Santiago, B.X., Surma, P., & Griffiths, R.E. 1996, ApJS, 107, 1
- Adams, F.C., Ruden, S.P., & Shu, F.H. 1989, ApJ 347, 959
- Adler, D.S., & Liszt, H.S. 1989, ApJ, 339, 836
- Alexander, R.D., Armitage, P.J., Cuadra, J., & Begelman, M.C. 2007, (arXiv 0711.0759)
- Alard, C. 2001, A&A, 379, L44
- Andersen, D.R., & Bershadsky, M.A. 2002, in "Disks of Galaxies: Kinematics, Dynamics and Perturbations", ASP Conference Proceedings, Vol. 275. Eds. E. Athanassoula, A. Bosma, and R. Muijca (San Francisco: Astronomical Society of the Pacific), p.39
- Andersen, D.R., Bershadsky, M.A., Sparke, L.S., Gallagher, J.S., Wilcots, E.M., van Driel, W., & Monnier-Ragaigne, D. 2006, ApJS, 166, 505
- Angiras, R.A., Jog, C.J., Omar, A., & Dwarakanath, K.S. 2006, MNRAS, 369, 1849
- Angiras, R.A., Jog, C.J., Dwarakanath, K. S., & Verheijen, M.A.W. 2007, MNRAS, 378, 276
- Athanassoula, L. 2002, ApJ, 569, L83

- Bacon, R., Emsellem, E., Monnet, G., & Nieto, J. L., 1994, *A&A*, 281, 691
- Bacon, R., Emsellem, E., Combes, F., Copin, Y., Monnet, G., & Martin, P. 2001, *A & A*, 371, 409
- Bailin, J., Simon, J. D., Bolatto, A.D., Gibson, B.K., & Power, C. 2007, *ApJ*, 667, 191
- Baldwin, J.E., Lynden-Bell, D., & Sancisi, R. 1980, *MNRAS*, 193, 313
- Bally, J., Stark, A. A., Wilson, R. W., & Henkel, C. 1988, *ApJ*, 324, 223
- Banerjee, A., & Jog, C.J. 2008, *ApJ*, 685, 254
- Barnes, J.E. 1992, *ApJ*, 393, 484
- Batcheldor D., Axon D., Merritt D. et al.: 2005, *ApJS* 160, 76
- Beale, J.S., & Davies, R.D. 1969, *Nature*, 221, 531
- Becquaert, J.-F., & Combes, F. 1997, *A & A*, 325, 41
- Begeman, K.G. 1987, Ph.D. thesis, University of Groningen
- Bekki, K. 2000a, *ApJ*, 540, L79
- Bekki, K. 2000b, *ApJ*, 545, 753
- Binney, J., & Tremaine, S. 1997, *Galactic Dynamics* (Princeton: Princeton Univ. Press)
- Block, D.L., Bertin, G., Stockton, A., Grosbol, P., Moorwood, A.F.M., & Peletier, R.F. 1994, *A & A*, 288, 365
- Block, D.L., Bournaud, F., Combes, F., Puerari, I., & Buta, R. 2002, *A & A*, 394, L35
- Block, D.L., Bournaud, F., Combes, F., Groess, R., Barmby, P., Ashby, M. L. N., Fazio, G. G., Pahre, M. A., & Willner, S. P. 2006, *Nature*, 443, 832
- Bontekoe, Tj. R., & van Albada, T. S. 1987, *MNRAS*, 224, 349
- Bosma, A. 1981, *AJ*, 86, 1791
- Bournaud, F., Combes, F., & Jog, C.J. 2004, *A & A*, 418, L27
- Bournaud, F., Jog, C.J., & Combes, F. 2005 a, *A & A*, 437, 69

- Bournaud, F., Combes, F., Jog, C.J., & Puerari, I. 2005 b, *A & A* , 438, 507
- Braun, R. 1995, *A & A S*, 114, 409
- Briggs, F. 1990, *ApJ*, 352, 15
- Buta, R., Vasylyev, S., Salo, H., & Laurikainen, E. 2005, *AJ*, 130, 506
- Chan, R. & Junqueira, S. 2003, *ApJ*, 586, 780
- Charlton J.C., & Laguna P. 1995, *ApJ*, 444, 193
- Chatterjee, P., Hernquist, L., & Loeb, A. 2002, *ApJ*, 572, 371
- Chemin, L., Cayattte, V., Carignan, C., Amram, P., Garrido, O., Hernandez, O., Maercelin, M., Adami, C., Boselli, A., & Boulesterix, J. 2006, *MNRAS*, 366, 812
- Chitre, A., & Jog, C.J. 2002, *A & A*, 388, 407
- Colin J., & Athanassoula E. 1981, *A&A*, 97, 63
- Combes, F. 2000, in *GH Advanced Lectures on the Starburst-AGN Connection*, INAOE, June 2000, ed. D. Kunth, I. Aretxaga (astro-ph/0010570)
- Combes, F., Boisse, P., Mazure, A., & Blanchard, A. 2004, "Galaxies & Cosmology" , second edition (Berlin: Springer-Verlag)
- Combes F., Leon S., & Meylan G. 1999, *A&A*, 352, 149
- Combes, F. 2008, in "Formation and Evolution of Galaxy Disks", ed. J. Funes & E. Corsini (arXiv:0801.0343)
- Comins, N.F., Lovelace, R. V. E., Zeltwanger, T., & Shorey, P. 1997, *ApJ*, 484, L33
- Conselice, C.J., Bershady, M.A., & Jangren, A. 2000, *ApJ*, 529, 886
- Davidge, T. J., Rigaut, F., Doyon, R., & Crampton, D. 1997, *AJ*, 113, 2094
- Davis, D.S., Keel, W.C., Mulchaey, J.S., & Henning, P.A. 1997, *AJ*, 114, 613
- Debattista, V., & Sambhus, N. 2008, preprint
- de Oliveira, M., & Combes, F. 2008, in preparation
- de Vaucouleurs G., & Freeman K.C. 1970, *IAU* 38, 356

- Downes, D., & Solomon, P.M. 1998, *ApJ*, 507, 615
- Dressler, A., & Richstone, D. O., 1988, *ApJ* 324, 701
- Dury, V. De Rijcke, S., Debattista, V.P., & Dejonghe H. 2008, *MNRAS*, 387, 2
- Earn D., & Lynden-Bell, D. 1996, *MNRAS*, 278, 395
- Elmegreen, D.M. & Elmegreen, B. G. 1982, *MNRAS*, 201, 1021
- Elmegreen, D.M., Elmegreen, B. G., & Hirst, A. C. 2004, *ApJ*, 604, L21
- Emsellem, E., & Combes, F., 1997, *A&A*, 323, 674
- Emsellem, E. , Cappellari M., Peletier R., McDermid, R.M., Bacon, R., Bureau, M., Copin, Y., Davies, Roger L., Krajnovic, D., Kuntschner, H. and 2 coauthors 2004, *MNRAS*, 352, 721
- Fuchs, B. 2004, *A & A*, 419, 941
- Gao, L., & White, S.D.M. 2006, *MNRAS*, 373, 65
- Garcia, M. R., Murray, S. S., & Primini, F. A. et al. 2000, *ApJ*, 537, 23
- Garcia-Burillo, S., Sempere, M. J., Combes, F., Hunt, L. K., & Neri, R. 2000, *A&A*, 363, 869
- Garcia-Burillo, S., Combes, F., Hunt, L. K. et al.: 2003, *A&A*, 407, 485
- Gebhardt, K., Bender, R., Bower, G. et al. 2000, *ApJ*, 539, L13
- Gentile, G., Burkert, A., Salucci, P., Klein, U., & Walter, F. 2005, *ApJ*, 634, L145
- Gerin M., Combes F., & Athanassoula E. 1990, *A&A*, 230, 37
- Giovanelli, R., & Haynes, M.P. in *Galactic and Extragalactic Radio Astronomy*, eds. G.L. Verschuur & K.I. Kellermann, Second edition, New York-Springer, 522
- Goldreich, P., & Tremaine, S., 1979, *AJ*, 84, 1638
- Gonzalez-Serrano J.I., & Carballo R. 2000, *A&AS*, 142, 353
- Haynes, M.P., Giovanelli, R., & Kent, B.R., 2007, *ApJ*, 665, L19
- Haynes, M.P., Hogg, D.E., Maddalena, R.J., Roberts, M.S., & van Zee, L.

- 1998, AJ, 115, 62
- Heemskerk, M. H. M., Papaloizou, J. C., & Savonije, G. J., 1992, A&A 260, 161
- Heller, A.B., Brosch, N., Almozino, E., van Zee, L., & Salzer, J. 2000, MNRAS, 316, 569
- Hozumi, S. & Fujiwara, T. 1989, PASJ, 41, 841
- Ibata, R., Irwin, M., Lewis, G., Ferguson, A. M. N., & Tanvir, N. 2001, Nature, 412, 49
- Ideta, M. 2002, ApJ, 568, 190
- Ideta, M., Hozumi, S., Tsuchiya, T., & Takizawa, M. 2000, MNRAS, 311, 733
- Irwin, M., Ferguson, A. M. N., Ibata, R., Lewis, G., & Tanvir, N. 2005, ApJ, 628, L105
- Jacobs, V., & Sellwood, J. A., 2001, ApJ, 555, L25
- Jarrett, T.H., Chester, T., Cutri, R., Schneider, S.E., & Huchra, J.P. 2003, AJ, 125, 525
- Jog, C.J. 1992, ApJ, 390, 378
- Jog, C.J. 1997, ApJ, 488, 642
- Jog, C.J. 1999, ApJ, 522, 661
- Jog, C.J. 2000, ApJ, 542, 216
- Jog, C.J. 2002, A & A, 391, 471
- Jog, C. J., & Maybhate, A. 2006, MNRAS, 370, 891
- Jog, C.J., & Solomon, P.M. 1992, ApJ, 387, 152
- Johnston K.V., Sigurdsson S., & Henquist L. 1999, MNRAS, 302, 771
- Junqueira, S. & Combes, F. 1996, A&A, 312, 703
- Kamphuis, P. 1993, Ph.D. thesis, University of Groningen.
- Kannappan, S.J., & Fabricant, D.G. 2001, AJ, 121, 140
- Kato, S. 1983, PASJ, 35, 248

- King, I. R., Stanford, S. A., & Crane, P., 1995, *AJ*, 109, 164
- Kormendy, J., 1988, *ApJ*, 325, 128
- Kormendy, J., & Bender, R., 1999, *ApJ*, 522, 772
- Kornreich, D.A., Haynes, M.P., & Lovelace, R.V.E. 1998, *AJ*, 116, 2154
- Kornreich, D.A., Lovelace, R.V.E., & Haynes, M.P. 2002, *ApJ*, 580, 705
- Kuijken, K. 1993, *ApJ*, 409, 68
- Kuijken, K., Fisher, D., & Merrifield, M.R. 1996, *MNRAS*, 283, 543
- Laine, S., & Heller, C.H. 1999, *MNRAS*, 308, 557 7479
- Lake, G., Katz, N. & Moore, B. 1998, *ApJ*, 495, 152
- Lallemant A., Duchesne M., & Walker M.F., 1960, *PASP*, 72, 76
- Lauer, T. R., Faber, S. M., Gebhardt K. et al 2005, *AJ*, 129, 2138
- Lauer, T. R., Gebhardt K., Richstone D. et al. 2002, *AJ*, 124, 1975
- Lauer, T. R., Faber, S. M., Ajhar, E. A., Grillmair, C. J., & Scowen, P. A., 1998, *AJ*, 116, 2263
- Lauer, T. R., Tremaine, S., Ajhar, E. A. et al. 1996, *ApJ*, 471, L79
- Lauer, T. R., Faber, S. M., Groth, E. J., et al. 1993, *AJ*, 106, 1436
- Laurikainen, E., Salo, H., & Rautiainen, P. 2002, *MNRAS*, 331, 880
- Lee E., & Goodman J. 1999, *MNRAS*, 308, 984
- Levine, E.S., Blitz, L., & Heiles, C. 2006, *ApJ*, 643, 881
- Levine, S.E., & Sparke, L.S. 1998, *ApJ*, 496, L13
- Light, E. S., Danielson, R. E., & Schwarzschild, M., 1974, *ApJ*, 194, 257
- Lin C.C., & Shu F.H. 1964, *ApJ*, 140, 646
- Lindblad, P. 1959, *Galactic Dynamics in Handbuch der Physics*, 53, 21
- Liszt, H. 2006, *A&A*, 447, 533
- Lord, S.D., & Young, J.S. 1990, *ApJ*, 356, 135

- Lovelace, R.V.E., Zhang, L., Kornreich, D.A., & Haynes, M.P., 1999, *ApJ*, 524, 634
- Lynden-Bell, D., & Kalnajs, A. 1972, *MNRAS*, 157, 1
- Makino, J., & Sugimoto, D. 1987, *PASJ*, 39, 589
- Manthey, E. et al. 2008, in preparation
- Mapelli, M., Moore, B., & Bland-Hawthorn, J. 2008, *MNRAS*, 388, 697
- Marshall, D.J., Fux R., Robin, A.C., & Reyl  , C. 2008, *A&A* 477, L21
- Masset, F., & Tagger, M. 1997, *A & A*, 332, 442
- Matthews, L.D., van Driel, W., & Gallagher, J.S. 1998, *AJ*, 116, 2196
- McDermid, R. M., Emsellem, E., Shapiro, K. L. et al. 2006, *MNRAS*, 373, 906
- Melchior, A-L., Viallefond, F., Guelin, M., & Neininger, N., 2000, *MNRAS* 312, L29
- Merritt, D., & Cruz, F. 2001, *ApJ*, 551, L41
- Miller, R.H., & Smith, B.F., 1992, *ApJ*, 393, 508
- Miller, R.H., & Smith, B.F., 1994, *CeMDA*, 59, 161
- Mould, J., Graham, J., Matthews, K., Soifer, B. T., & Phinney, E. S. 1989, *ApJ*, 339, L21
- Narayan, C.A., Saha, K., & Jog, C.J. 2005, *A & A*, 440, 523
- Natarajan, P. 2002, The shape of the galaxies and their dark halos, Yale cosmology workshop (Singapore: World Scientific)
- Nelson, R.W., & Tremaine, S.D. 1995, *MNRAS*, 275, 897
- Nieto, J.-L., Macchetto, F. D., Perryman, M. A. C., di Serego Alighieri, S., & Lelievre, G. 1986, *A&A*, 165, 189
- Nishiura, S., Shimada, M., Ohyama, Y., Murayama, T., & Taniguchi, Y. 2000, *AJ*, 120, 1691
- Noordermeer, E., Sparke, L., & Levine, S.E. 2001, *MNRAS*, 328, 1064
- Noordermeer, E., van der Hulst, J. M., Sancisi, R., Swaters, R. A., & van Albada, T. S. 2005, *A&A* 442, 137

- Olling, R.P. 1996, AJ, 112, 481
- Pasha, I.I. 1985, Soviet Astr. Letters, 11, 1
- Peiris H., & Tremaine S. 2003, ApJ 599, 237
- Phookun B., & Mundy L.G. 1995, ApJ, 453, 154
- Phookun, B., Vogel, S.N., & Mundy, L.G. 1993, ApJ, 418, 113
- Pranav, P., & Jog, C.J. 2008, in preparation.
- Quillen A. C., & Hubbard A. 2003, AJ, 125, 2998
- Rauch K.P., & Tremaine S. 1996, New A., 1, 149
- Reichard, T.A., Heckman, T.M., Rudnick, G., Brinchmann, J., & Kauffmann G. 2008, ApJ, 677, 186
- Reshetnikov, V., & Combes, F. 1998, A & A, 337, 8
- Richmond, M.W., & Knapp, G.R. 1986, AJ, 91, 517
- Richter O.-G., & Sancisi, R. 1994, A & A, 290, L9
- Rix, H.-W., & Rieke, M.J. 1993, ApJ, 418, 123
- Rix, H.-W., & Zaritsky, D. 1995, ApJ, 447, 82
- Rodriguez-Fernandez N., & Combes F. 2008, A&A, 489, 115
- Rohlf, K. 1977, Lecture notes on density wave theory, (Berlin: Springer-Verlag)
- Rubin, V.C., Hunter, D.A., & Ford, W.K. Jr. 1991, ApJS, 76, 153
- Rubin, V.C., Waterman, A.H., & Kenney, J. D. 1999, AJ, 118, 236
- Rudnick, G. & Rix, H.-W. 1998, AJ, 116, 1163
- Sackett, P.D., & Sparke, L.S. 1990, ApJ, 361, 408
- Sage, L.J., & Solomon, P.M. 1991, ApJ, 380, 392
- Saha, K., Levine, E., Jog, C.J., & Blitz, L. 2008, ApJ, submitted.
- Saha, K. 2008, MNRAS, 386, L101



- Saha, K., Combes, F., & Jog, C.J. 2007, MNRAS, 382, 419
- Saha, K., & Jog, C.J. 2006, MNRAS, 367, 1297
- Sakamoto K., Matsushita S., Peck A. et al. 2004, ApJ, 616, L59
- Salow, R.M., & Statler, T.S. 2004, ApJ, 611, 245
- Salow, R.M., & Statler, T.S. 2001, ApJ, 551, L49
- Sambhus, N., & Sridhar, S. 2002, A&A 388, 766 R
- Sancisi, R., Fraternali, F., Oosterloo, T., & van der Hulst J.M. 2008, Astronomy & Astrophysics Reviews (arXiv0803.0109)
- Sandage, A. 1961, The Hubble Atlas Of Galaxies (Washington: Carnegie Institution Of Washington)
- Schoenmakers, R.H.M. 1999, Ph.D. thesis, University of Groningen.
- Schoenmakers, R.H.M. 2000, in Small Galaxy Groups, eds. Valtonen, M. & Flynn, C., ASP conf. series vol. 209, pg. 54
- Schoenmakers, R.H.M., Franx, M., & de Zeeuw, P.T. 1997, MNRAS, 292, 349
- Schweizer, F. 1996, AJ, 111, 109
- Sellwood, J.A., & Valluri, M. 1997, MNRAS, 287, 124
- Semelin, B. & Combes, F. 2005, A & A, 441, 55
- Shlosman, I. 2005, in The Evolution of Starbursts, Eds. S. Huettemeister and E. Manthey (Melville: AIP) (astro-ph/0412163)
- Shu F.H., Tremaine S., Adams F.C., & Ruden S.P., 1990, ApJ, 358, 495
- Simard, L., Willmer, C. N. A., Vogt, N. P. et al. 2002, ApJS, 142, 1
- Sofue, Y. & Rubin, V. 2001, ARAA, 39, 137
- Statler, T. S., King, I. R., Crane, P., and Jedrzejewski, R. I. 1999, AJ, 117, 894
- Statler, T. 2001, AJ, 122, 2257
- Swaters, R.A., Schoenmakers, R.H.M., Sancisi, R., & van Albada, T.S. 1999, MNRAS, 304, 330

- Swaters, R.A., van Albada, T.S., van der Hulst, J.M., & Sancisi, R. 2002, A & A, 390, 829
- Swaters, R.A. 1999, Dark matter in late-type dwarf galaxies, Ph.D. thesis, University of Groningen.
- Sweatman W.L. 1993, MNRAS 261, 497
- Syer, D., & Tremaine, S., 1996, MNRAS, 281, 925
- Taga, M., & Iye, M. 1998a, MNRAS, 299, 111
- Taga, M., & Iye, M. 1998b, MNRAS, 299, 1132
- Thatte N., Tecza M., & Genzel R. 2000, A&A, 364, L47
- Thomasson, M., Donner, K.J., Sundelius, B., Byrd, G.G., Huang, T.-Y., & Valtonen, M.J. 1989, A & A, 211, 25
- Toomre, A. 1981, in Structure & Evolution of normal galaxies, eds. S.M. Fall & D. Lynden-Bell (Cambridge: Cambridge Univ. Press)
- Toth, G., & Ostriker, J.P. 1992, ApJ, 389, 5
- Touma J. 2002, MNRAS, 333, 583
- Tremaine, S.D., Ostriker J.P., & Spitzer L. 1975, ApJ, 196, 407
- Tremaine, S. 1995, AJ, 110, 628
- Tremaine S. 2001, AJ, 121, 1776
- Tremaine S. 2005, ApJ, 625, 143
- Verheijen, M.A.W. 1997, Ph.D. thesis, University of Groningen
- Vesperini, E., & Weinberg, M.D. 2000, ApJ, 534, 598
- Vollmer, B., Braine, J., Balkowski, C., Cayatte, V., & Duschl, W. J. 2001, A & A, 374, 824
- Walker, I. R., Mihos, J.C., & Hernquist, L. 1996, ApJ, 460, 121
- Weinberg, M.D. 1994, ApJ, 421, 481
- Weinberg, M.D. 1995, ApJ, 455, L31
- Weinberg, M.D. 1998, MNRAS 299, 499

Wilcots, E. M., & Prescott, M.K.M. 2004, AJ, 127, 1900

Wilson, A.S., & Baldwin, J.A. 1985, ApJ, 289, 124

Woodward, J.W., Tohline, J.E., & Hachisu, J. 1994, ApJ, 420, 247

Young, J.S. 1990, in The Interstellar Medium in Galaxies, eds. H.A. Thronson and M.J. Shull, Kluwer: Dordrecht, pg. 67

Young, L.M., Rosolowski, E., van Gorkom, J.H., & Lamb, S.A. 2006, ApJ, 650, 166

Zaritsky, D., & Rix, H.-W. 1997, ApJ, 477, 118